Aging and Alzheimer's Disease Have Dissociable Effects on Medial Temporal Lobe Connectivity

Stanislau Hrybouski[1,2], Sandhitsu R. Das[1,3,4,5], Long Xie[1,2,6], Laura E. M. Wisse[1,2,7], Melissa Kelley[4], Jacqueline Lane[4], Monica Sherin[4], Michael DiCalogero[4], Ilya Nasrallah[2,5], John A. Detre[2,3], Paul A. Yushkevich[1,2,5], and David A. Wolk[3,5]

[1]Penn Image Computing and Science Laboratory (PICSL), University of Pennsylvania, Philadelphia, Pennsylvania; [2]Department of Radiology, University of Pennsylvania, Philadelphia, Pennsylvania; [3]Department of Neurology, University of Pennsylvania, Philadelphia, Pennsylvania; [4]Penn Memory Center, University of Pennsylvania, Philadelphia, Pennsylvania; [5]Penn Alzheimer's Disease Research Center, University of Pennsylvania, Philadelphia, Pennsylvania; [6]Siemens Healthineers, Digital Technology and Innovation, Princeton, New Jersey; [7]Department of Diagnostic Radiology, Lund University, Lund, Sweden

Correspondence

David A. Wolk, #507, Goddard, 3710 Hamilton Walk, Philadelphia, PA 19104. Phone: (215)-662-7810; e-mail: david.wolk@pennmedicine.upenn.edu

ABSTRACT

Functional disruption of the medial temporal lobe-dependent networks is thought to underlie episodic memory deficits in aging and Alzheimer's disease. Previous studies revealed that the anterior medial temporal lobe is more vulnerable to pathological and neurodegenerative processes in Alzheimer's disease. In contrast, cognitive and structural imaging literature indicates posterior, as opposed to anterior, medial temporal lobe vulnerability in normal aging. However, the extent to which Alzheimer's and aging-related pathological processes relate to functional disruption of the medial temporal lobe-dependent brain networks is poorly understood. To address this knowledge gap, we examined functional connectivity alterations in the medial temporal lobe and its immediate functional neighborhood – the Anterior-Temporal and Posterior-Medial brain networks – in normal agers, individuals with preclinical Alzheimer's disease, and patients with Mild Cognitive Impairment or mild dementia due to Alzheimer's disease. In the Anterior-Temporal network and in the perirhinal cortex, in particular, we observed an inverted 'U-shaped' relationship between functional connectivity and Alzheimer's stage. According to our results, the preclinical phase of Alzheimer's disease is characterized by increased functional connectivity between the perirhinal cortex and other regions of the medial temporal lobe, as well as between the anterior medial temporal lobe and its one-hop neighbors in the Anterior-Temporal system. This effect is no longer present in symptomatic Alzheimer's disease. Instead, patients with symptomatic Alzheimer's disease displayed reduced hippocampal connectivity within the medial temporal lobe as well as hypoconnectivity within the Posterior-Medial system. For normal aging, our results led to three main conclusions: (1) intra-network connectivity of both the Anterior-Temporal and Posterior-Medial networks declines with age; (2) the anterior and posterior segments of the medial temporal lobe become increasingly decoupled from each other with advancing age; and, (3) the posterior subregions of the medial temporal lobe, especially the parahippocampal cortex, are more vulnerable to age-associated loss of function than their anterior counterparts. Together, the current results highlight evolving medial temporal lobe dysfunction in Alzheimer's disease and indicate different neurobiological mechanisms of the medial temporal lobe network disruption in aging vs. Alzheimer's disease.

Keywords: functional connectivity; medial temporal lobe; AT network; PM network; Alzheimer's disease; aging

Abbreviations: AD = Alzheimer's disease; AT = anterior-temporal; BOLD = blood oxygen level-dependent; CI = cognitively impaired; CU = cognitively unimpaired; ERC = entorhinal cortex; FC = functional connectivity; fMRI = functional MRI; HP = hippocampus; MTL = medial temporal lobe; PM = posterior-medial; PHC = parahippocampal cortex; PRC = perirhinal cortex

INTRODUCTION

Structures of the Medial Temporal Lobe (MTL) have attracted extensive scientific inquiry for over fifty years because of this region's role not only in episodic memory but also in the processing of emotional content, social cognition, creative thought, short-term memory, and object discrimination.[1-10] Both human and animal studies implicate the MTL as the key region involved in memory decline in aging and Alzheimer's disease (AD).[11-14]

Core memory-associated MTL subregions are the hippocampus (HP) and the perirhinal (PRC), entorhinal (ERC), and parahippocampal (PHC) cortices.[6,7,13] Although unresolved, there is considerable evidence that the functional organization of the MTL can be divided along the anterior-posterior axis.[6,7,15] Further, a growing body of clinical literature indicates the differential vulnerability of the anterior vs. posterior MTL to atrophy and pathological processes.[16-20] The anterior MTL consists of the anterior HP (primarily head), PRC, and ERC, while the posterior MTL consists of the posterior (body + tail) HP and PHC. Because the MTL is one of the most densely connected regions in the brain,[21] MTL dysfunction is likely to propagate to extra-MTL brain areas with which various MTL subregions interact. Thus, changes in MTL function ought to be considered in the context of their functional communities. Two brain networks have been hypothesized to explain MTL-cortical interactions: the Anterior-Temporal (AT) and Posterior-Medial (PM).[6,22-25] The anterior MTL regions (i.e., PRC, ERC, anterior HP, and amygdala) belong to the AT network, which also includes a number of extra-MTL regions such as lateral temporal and orbitofrontal cortices, and the temporal pole.[6] The PM network consists of the posterior MTL (i.e., posterior HP and PHC, but sometimes also includes medial ERC) along with a number of medial parietal regions, especially the posterior cingulate, precuneus, and retrosplenial.[6,26] In AD, tau pathology is more pronounced in the AT network, while amyloid plaques are more prevalent in the PM network.[24,27]

MTL dysfunction is an early feature of AD,[11,12,28-31] corroborated by previous task-based functional neuroimaging studies which reported increased HP activation in patients with Mild

Cognitive Impairment (MCI),[32-36] and in individuals at genetic risk for AD, including asymptomatic carriers of the apolipoprotein ε4 allele.[37-42] Results from functional connectivity (FC) studies have been less clear with mixed findings of both increased and decreased MTL connectivity in patients with MCI or dementia-level impairment due to AD.[22,43-47] In addition, changes in the MTL function at the systems level in normal aging are largely unexplored, and despite their relevance to declining memory in aging and AD, the network architecture of the AT and PM systems has not been precisely mapped. Given these knowledge gaps in the field, the primary aim of our current study was to determine whether and how age-associated FC changes within the MTL, and its immediate functional neighborhood – AT and PM network systems – differ from those that are caused by AD, especially during the earliest preclinical stage of the disease, when clinical interventions have the greatest potential. Our secondary goal was to construct detailed maps of MTL-associated networks.

As suggested by animal models of AD that revealed amyloid-induced hyperexcitability within the MTL circuitry, including subclinical seizures, during the early stages of the disease,[48-54] we predicted MTL hyperconnectivity in individuals with preclinical AD. Since animal work has also demonstrated the activity-dependent nature of tau accumulation and spread,[49,55] we hypothesized that the aforementioned hyperconnectivity effect would be most prominent in the anterior MTL – and the PRC in particular – because this region includes the transentorhinal cortex, the earliest locus of tau pathology in AD.[12,14,17,21,56] Furthermore, because rising tau is associated with synapse loss, cell death, and circuit breakdown,[57-59] we predicted that symptomatic stages of AD would be characterized by reduced, not excessive, FC levels. In normal aging, we expected to see a generalized loss of network integrity, consistent with previous observations in other systems,[60-66] but perhaps more prominently in the PM network given more robust declines in cognitive function ascribed to this network in prior studies of cognitive aging.[6,7,67-71]

MATERIALS AND METHODS

Participants

In this cross-sectional study, we analyzed data from 179 individuals from the Aging Brain Cohort (ABC) study of the University of Pennsylvania Alzheimer's Disease Research Center (Penn ADRC). These participants undergo annual cognitive evaluations, including psychometric testing as prescribed by the Uniform Data Set 3.0.[72] Consensus diagnoses are reached by a team that includes neurologists and neuropsychologists using clinical history and cognitive scores. Amyloid status was determined by a visual read of amyloid PET scans (see below for acquisition parameters). An additional group of younger adults (< 60 years of age) were recruited beyond the ABC study to capture the full adult age span. Thus, four groups were formed: (1) 36 cognitively unimpaired (CU) participants < 60 years of age were classified as *normal young and middle-aged adults* [age range 23-59 years; mean Montreal Cognitive Assessment (MoCA)[73] total score $\pm$ SD = 26.1 $\pm$ 3.7], (2) 80 Aβ-negative CU participants > 60 years of age were classified as *normal older adults* [age range 63-86 years; mean MoCA $\pm$ SD = 27.4 $\pm$ 2.0], (3) 23 A β-positive CU participants > 60 years of age were categorized as *preclinical AD* [age range = 65-87 years; mean MoCA $\pm$ SD = 26.9 $\pm$ 1.6], and (4) 40 Aβ-positive cognitively impaired (CI) participants were categorized as *symptomatic AD* [age range 57-87 years; mean MoCA $\pm$ SD = 20.3 $\pm$ 4.2]. In all analyses aimed at studying the effects of normal aging on MTL connectivity, the first two groups (i.e., normal young, middle-aged, and older adults) were merged into a single *normal agers* cohort. Additional information about our participants is presented in Table 1. The study was approved by the University of Pennsylvania Institutional Review Board.

Table 1: Demographic information for each group in the study. Amyloid-PET standard uptake value ratio (SUVR) is shown for the Florbetaben tracer only.

	Young & Middle-Aged (*N* = 36)	Aβ− CU (*N* = 80)	Aβ+ CU (*N* = 23)	Aβ+ CI (*N* = 40)
Age (years)				
Mean ± SD	39.2 ± 11.8	71.1 ± 4.9	75.2 ± 6.0	71.7 ± 6.9
Range [min/max]	23/59	63/86	65/87	57/87
Race (White/Black/Asian/Other)	20/12/3/1	61/17/0/2	21/2/0/0	35/4/0/1
Sex (males/females)	14/22	29/51	7/16	23/17
Education (years) ± SD	16.2 ± 2.6	16.6 ± 2.6	16.9 ± 1.7	16.5 ± 2.6
Total MoCA ± SD	26.1 ± 3.7	27.4 ± 2.0	26.9 ± 1.6	20.2 ± 4.3
CDR (sum/global)	N/A	0.038/0.031	0.087/0.065	2.962/0.638
Composite Aβ SUVR ± SD (Florbetaben *n*)	N/A	0.950 ± 0.062 (*n* = 68)	1.280 ± 0.201 (*n* = 21)	1.438 ± 0.144 (*n* = 37)

Image Acquisition

All structural and functional MRI datasets were acquired using a 3.0 T Siemens Prisma scanner (Erlangen, Germany) at the Center for Advanced Magnetic Resonance Imaging and Spectroscopy (University of Pennsylvania, Philadelphia, PA). During a resting-state functional MRI (rs-fMRI) scan, 420 functional volumes were collected axially using a T2*-sensitive Gradient Echo Planar Imaging (EPI) pulse sequence sensitive to blood oxygenation level-dependent (BOLD) contrast [repetition time (TR): 720 ms; echo time (TE): 37 ms; flip angle: 52°; field of view (FOV): 208×208 mm^2; voxel size: 2×2×2 mm^3; 72 interleaved slices; phase encoding direction: anterior to posterior; partial *k*-space: 7/8; multi-band acceleration factor: 8]. A whole-brain T1-weighted 3D Magnetization Prepared Rapid Gradient Echo (MPRAGE) sequence [TR: 2400 ms; TE: 2.24 ms; inversion time: 1060 ms; flip angle: 8°; FOV: 256×240×167 mm^3; voxel size: 0.8×0.8×0.8 mm^3] was used to acquire anatomical images for MTL subregion segmentation and registration to template space. To estimate B_0 inhomogeneity, gradient echo field maps were also collected [TR: 580 ms; TE1/TE2: 4.12/6.58 ms; flip angle: 45°; FOV: 240×240 mm^2; voxel size: 3×3×3 mm^3; 60 interleaved slices].

Furthermore, all CU participants who were 60 years of age or older and all patients with symptomatic MCI or early AD underwent amyloid PET scanning. Our amyloid PET protocol used an injection of 8.1 mCi ± 20% of ^{18}F-Florbetaben or 10 mCi ± 20% for ^{18}F-Florbetapir and a 20 min brain scan (4 frames of 5-minute duration) following a standard uptake phase (a 90-min for ^{18}F-Florbetaben and 50 min for ^{18}F-Florbetapir). 44% of PET scans were acquired within six months of fMRI and 85% within a year of fMRI. Cognitively normal young and middle-aged adults underwent rs-fMRI but not PET imaging because this age group is unlikely to have measurable amyloid pathology.

Image Preprocessing

Initial processing of structural and functional images was performed on the Flywheel Imaging Informatics Platform (http://flywheel.io). We used a customized *fMRIprep* 20.0.7[74] analysis gear, which consisted of *mcflirt* realignment,[75,76] susceptibility distortion correction using a custom workflow of *SDCFlows*,[77] functional-to-structural boundary-based rigid-body registration,[78] SyN diffeomorphic registration to the 2-mm MNI152 template using Advanced Normalization Tools (ANTs),[79,80] followed by volumetric smoothing with a 6-mm FWHM Gaussian kernel, and decomposition of the fMRI time series into signal sources using the Probabilistic Spatial Independent Component Analysis (ICA).[81]

Next, manual ICA-based denoising was performed by a single rater (SH) with the aid of the automated movement component classifier, ICA-AROMA.[82] Protocols and reliability of manual ICA-based artifact detection have been detailed elsewhere.[64,83,84] Following the ICA-based denoising, the first 10 time points were discarded, and the rest of the fMRI pre-processing was done in the Conn toolbox (v. 20.b)[85] for MATLAB (release 2020b; The MathWorks Inc., Natick, MA). Rather than employing global signal regression, which can introduce artifactual anti-correlations into the fMRI time series,[86-88] we used 32 CompCorr[89] regressors – 16 from the White Matter (WM) and 16 from the cerebrospinal fluid (CSF) – that were extracted from the partially de-noised fMRI data using eroded tissue probability maps. Those 32 CompCorr regressors were supplemented with movement regressors based on the Friston 24-Parameter

model[90] as well as low-frequency sine and cosine waves (6 waveforms with periods of π, 2π, and 3π over 410 fMRI volumes) that were included to account for slow BOLD signal drifts. Since realignment parameters in sub-second fMRI acquisitions are contaminated by breathing-associated magnetic field perturbations,[91,92] those parameters were filtered using MATLAB scripts provided by Gratton *et al.*[91] prior to being used as nuisance covariates. In the last step of our pre-processing pipeline, the fMRI time series were band-pass filtered (0.008-0.150 Hz) and underwent linear detrending. Descriptions of our *fMRIprep* structural pipeline as well as our amyloid-PET preprocessing pipeline are provided in the Supplementary Materials.

The MTL subregions were segmented using the automated segmentation of hippocampal subfields-T1 (ASHS-T1) pipeline.[93] We used ASHS-T1 to generate Brodmann Area 36 (BA36), Brodmann Area 35 (BA35), ERC, PHC, as well as the anterior and posterior HP (aHP and pHP, respectively) segmentations. Because the theoretical framework tends to treat the PRC as a single functional unit,[6] we merged the BA35 and BA36 ROIs into a single PRC ROI. For visual reference, a single participant's ASHS-T1 segmentation is shown in Fig. 1a. Each subject's ASHS-T1 MTL segmentations were then registered to MNI space using the same deformation fields that were used to register that subject's fMRI data to the 2-mm MNI152 template. The warped ASHS-T1 ROIs were used to extract the denoised fMRI time series from each memory-related region of the MTL.

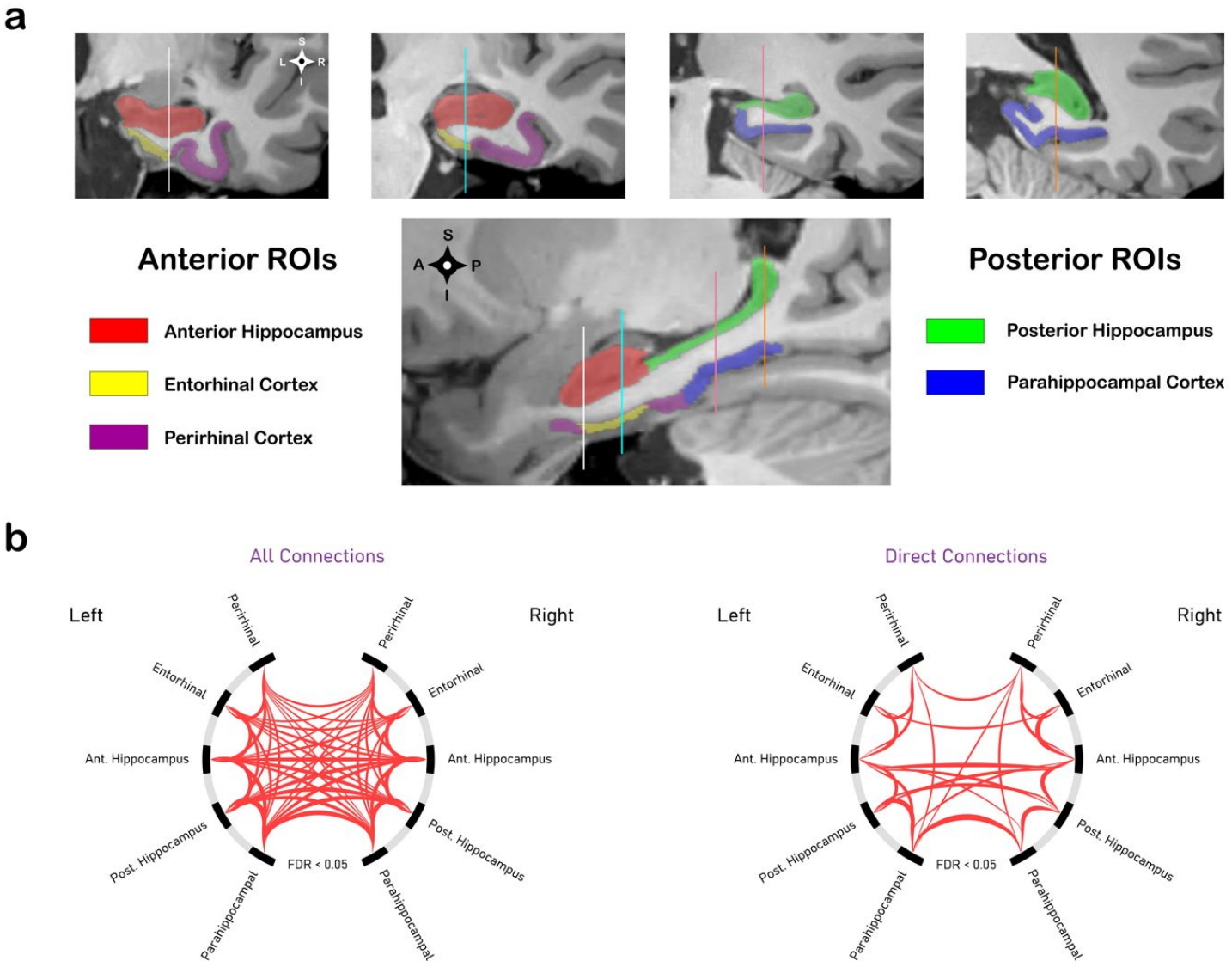

Figure 1. MTL subregions and their functional interactions with each other. **(a)** An example of MTL segmentation using ASHS-T1 pipeline; **(b)** Intra-MTL functional connectivity profiles in Aβ-negative cognitively normal adults. The connectogram on the left is based on correlational connectivity matrices, which do not control for indirect paths. The connectogram on the right is based on partial correlation matrices and represents direct functional interactions amongst various MTL subregions. Edge thickness in both connectograms is proportional to *t*-scores. Abbreviations: MTL = medial temporal lobe; FDR = false discovery rate.

Intra-MTL Functional Connectivity Analyses

The most common technique for modeling the brain's functional architecture is to use the bivariate Pearson correlation coefficient as a proxy for FC between brain regions.[94,95] Despite its high sensitivity, this approach may produce biased connectivity estimates because it does not control for indirect paths.[95,96] Such problems can be ameliorated by replacing bivariate correlation coefficients with partial correlations, controlling for signals from all other ROIs in the network model. However, the improvement in architectural accuracy comes at a price: noisier connectivity estimates and reduced statistical power when studying group effects.[96] Because each FC metric has a unique set of trade-offs, we examined the effects of age and AD pathology on intra-MTL FC using both approaches.

All statistical analyses of intra-MTL FC were performed using the Network-Based Statistics (NBS) toolbox.[97] The following NBS settings were used: (1) uncorrected connection-level *t*-statistic threshold was set to match two-tailed $p < 0.05$; (2) the cluster-mass 'intensity' option in the NBS algorithm was turned on; (3) positive and negative contrasts were run separately, and family-wise error (FWE)-corrected significance threshold was set at $p < 0.025$ for each one-sided (i.e., positive or negative) test; (4) 25,000 Freedman and Lane[98] permutations were used to construct each cluster-mass distribution under the null hypothesis. Prior to performing age effect analyses and group comparisons of intra-MTL FC, correlation matrices were Fisher Z-transformed, and overall intra-MTL connectivity maps were generated using all participants from the *normal agers* cohort [positive-sided one-sample connection-level *t*-tests with the False Discovery Rate (FDR)[99] correction for multiple comparisons]. These overall connectivity maps were used to select edges of interest (Fig. 1b). Since all MTL ROIs were functionally related to each other in the bivariate correlational method, all pairwise connections between ASHS-T1 ROIs were examined for the effects of age and AD pathology (Fig. 1b, left panel). For partial correlations, the above test identified 23 (out of 45) edges representing direct functional interactions within the MTL (Fig. 1b, right panel). In all subsequent intra-MTL FC analyses that used partial correlations, only those 23 edges were studied.

To study the effects of age on intra-MTL FC, we ran a General Linear Model (GLM) on FC data from the *normal agers* cohort with sex and 4 aggregate head movement metrics [mean filtered framewise displacement (FD), maximum filtered FD, mean DVARS, max DVARS; see Power *et al.*[100] for metric details] as nuisance covariates. To examine how MTL function differs between normal agers and individuals at different stages of AD progression, we performed all pairwise group comparisons of intra-MTL connectivity between *normal older adults*, *preclinical AD*, and *symptomatic AD*. In these group comparisons, age, sex, and aggregate head movement metrics were used as covariates. Connection-specific and supplementary statistical comparisons were performed using SPSS v. 28 (IBM Inc., Armonk, NY).

Identification of Cortical Regions with Functional Connectivity to the Medial Temporal Lobe

Seminal work by Braak and Braak[17] demonstrated that tau neurofibrillary tangle (NFT) pathology originates at the border of the PRC and ERC in the anterior MTL, and a recent *ex vivo* study by our group revealed the presence of an anterior-posterior NFT gradient within the MTL with posterior subregions being less vulnerable to NFT accumulation.[20] Regions with higher/lower NFT burden scores had a remarkable degree of spatial overlap with the MTL portion of the AT/PM network, and together with the AT network's vulnerability to tauopathy vs. PM network's vulnerability to amyloidosis, seem to reflect partially dissociable patterns of molecular pathology within the anterior vs. posterior MTL and might also relate to dissociable patterns of network disruption in the AT vs. PM system.[6,22,24,27] Thus, when modeling MTL interactions with the rest of the cortex, we employed four tau-based MTL ROIs (left/right $\times$ anterior/posterior). Our group recently built a novel atlas of MTL NFT accumulation using fusion of *ex vivo* MRI and serial histological imaging (Suppl. Fig. 1).[20] Left and right tau-based MTL ROIs were defined by thresholding and binarizing this NFT accumulation map (inclusion threshold: WildCat-based metric of NFT burden > 0.2; for threshold details see Yushkevich *et al.*),[20] and the anterior/posterior split was defined using the aHP/pHP boundary of the ASHS-T1 protocol.[7,93,101] Next, we identified cortical regions with positive FC to at least one of the four

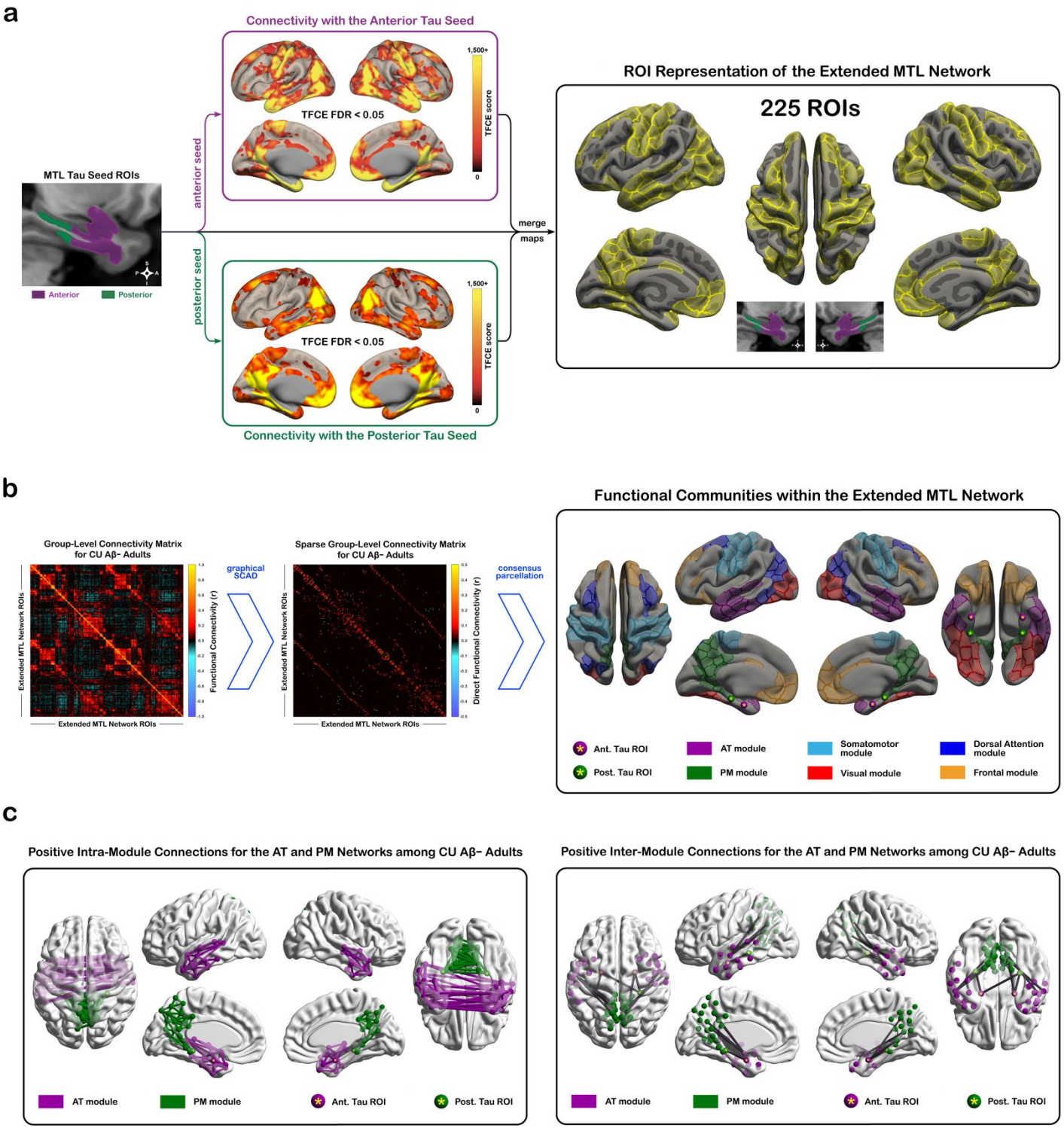

Figure 2. AT and PM network estimation. **(a)** Simplified schematic of the methodology that was used to select cortical regions that constitute the extended MTL network. Cortical regions with positive functional connectivity to the anterior or posterior tau-based MTL ROIs were identified and mapped onto ROI-based representation. **(b)** MTL network structure was estimated using graphical SCAD with BIC-based model selection. Functional modules within the extended MTL network were identified using consensus Louvain modularity. **(c)** AT and PM network architecture in the *normal agers* group (i.e., CU young, middle-aged, and Aβ-negative older participants). Left panel depicts the intra-module connections of each network; right panel depicts AT-PM inter-module connections. Abbreviations: AT = anterior-temporal; PM = posterior-medial; MTL = medial temporal lobe; CU = cognitively unimpaired; Ant. = anterior; Post. = posterior; TFCE = threshold-free cluster enhancement; FDR = false discovery rate; SCAD = smoothly clipped absolute deviation estimator.

tau-based MTL ROIs in the *normal agers* cohort (Fig. 2a). In ROI form, this extended MTL network was represented by the anterior and posterior tau-based MTL ROIs ($aMTL_{tau}$ and $pMTL_{tau}$, respectively) and 221 ROIs from the 400-region 17-Network Schaefer *et al.*[102] parcellation (Fig. 2a; Suppl. Materials).

Estimating MTL Network Architecture

The functional architecture of the extended MTL network was estimated using the graphical SCAD algorithm.[103-106] Similar to other sparse estimation techniques, graphical SCAD eliminates spurious or indirect connections by penalizing excessive model complexity if there is a lack of evidence in the data to support a more complex graph. Because sparse network estimation based on 225 ROIs and a relatively short fMRI acquisition is unlikely to produce sufficiently stable connectome estimates at the subject level, we performed group-level sparse network estimation instead. First, bivariate correlation matrices were computed for all *normal agers*. Those correlation matrices were then Fisher-transformed and averaged such that each decade of human lifespan had equal weight on the final connectivity structure. The resulting average Z-connectivity matrix was converted into the correlational connectivity matrix and used as the covariance source in SCAD-based network estimation (Fig. 2b). Graphical SCAD relies on two tuning parameters: α and ρ. To minimize the Bayes risk, Fan and Li[104] recommend $\alpha = 3.7$. The second tuning parameter, ρ, was selected from a set of $\rho = \{e^{-8.0}, e^{-7.8}, e^{-7.6}, \ldots, e^{0}\}$ by minimizing the Bayesian Information Criterion (BIC).[105,106] Custom MATLAB scripts, employing the QUIC optimizer,[107] were used to solve the graphical SCAD problem (Fig. 2b; Suppl. Materials).

To identify the AT and PM network communities within the broader MTL connectome, we used the two-sided Louvain modularity algorithm that incorporates both positive and negative edge weights in its community search.[108,109] Since modularity-based network parcellations can produce inconsistent networks from one iteration to another, we built a consensus parcellation from 5,000 separate iterations of the fine-tuned two-sided Louvain community search.[109-111] Module detection was performed on the *normal agers'* sparse partial correlation matrix

estimated above. In total, we identified 6 stable functional modules that could explain functional relationships among the 225 MTL-affiliated ROIs (Fig. 2b). Two of those modules were consistent with the AT and PM networks that have been reported in the literature.[6] The parcellation procedure was performed using functions from the Brain Connectivity Toolbox.[112]

Statistical Analyses of Intra-AT, Intra-PM, and AT-PM Connectivity

Age effect analyses and AD group comparisons were performed on bivariate connectivity matrices, but only on those connections that survived group-level graphical SCAD estimation in at least one test-related group. For age effect analyses, in addition to the overall connectivity map that was estimated above, we also estimated separate SCAD-based maps for younger (*normal agers* < 60 years) and older (*normal agers* > 60 years) participants. If a connection was positive in at least one of the three (i.e., younger, older, overall) group-level sparse connectivity matrices, it was examined for age effects. Negative edges and those with conflicting signs in the bivariate vs. graphical SCAD models were excluded because of interpretability issues. The final set of intra-AT, intra-PM, and AT-PM connections that were used in age effect analyses is shown in Fig. 2c. For AD group comparisons, similar criteria were used, except that there were 2 instead of 3 group-level connectivity estimates per comparison. For example, for the preclinical vs. symptomatic AD connectivity comparison, two separate group-level graphical SCAD connectivity estimates were computed: the first for the preclinical group and the second for the symptomatic group.

Statistical analyses of the AT and PM intra-module and AT-PM connectivity were performed using the NBS GLM approach[97] with all settings, including covariates, matching those that were used in the intra-MTL analyses described above. Connection-specific follow-up comparisons were performed using SPSS v. 28 (IBM Inc., Armonk, NY). All AT and PM network results were visualized with the BrainNet Viewer.[113]

Data Availability

Anonymized preprocessed data and in-house analysis scripts will be made available upon request for the sole purpose of replicating procedures and results presented in this article.

RESULTS

Effects of Age and AD Progression on Functional Connectivity between the MTL Subregions

The NBS algorithm identified a single cluster of 14 edges that represents declining FC in *normal agers* (FWE $p < 0.01$; Fig. 3a). Most of the cluster's connections were interhemispheric (10 out of 14 edges), and all but one represented either anterior-with-posterior or posterior-with-posterior functional interactions. The PHC was involved in 9 out of 14 connections with a negative correlation to age. We did not observe any positive associations between age and intra-MTL FC.

Comparing intra-MTL connectivity profiles of the Aβ− CU and Aβ+ CU older adult groups revealed increased functional coupling between the right PRC and other MTL subregions in the preclinical AD group (Fig. 3b). Although PRC hyperconnectivity reached statistical significance in the right hemisphere only, similar trends were observed in the left hemisphere as well (Fig. 3e). To test whether these alterations in MTL function were linked to structural atrophy in the MTL, we used two-way ANCOVAs [Group and Sex as fixed factors; Age as a covariate] to compare the Aβ− CU vs. Aβ+ CU groups MTL volumetric measurements (thickness for PRC, ERC, and PHC; ICV-corrected volumes for aHP and pHP; thickness/volumes averaged across hemispheres). Because we did not detect any significant differences in MTL structure when comparing normal older adults to individuals with preclinical AD (all p values > 0.10), we concluded that MTL network dysfunction likely precedes neuronal loss in AD.

To investigate the effects of disease progression on the MTL function, we compared intra-MTL connectivity profiles of the Aβ+ CI group to those of the age-matched Aβ− CU and Aβ+ CU groups. Relative to normal older adults, individuals in the Aβ+ CI group displayed lower hippocampal connectivity (Fig. 3c), suggesting that functional changes in the symptomatic disease are characterized by functional decoupling of the two hippocampi from each other and from the rest of the MTL. Contrasting intra-MTL connectivity profiles of the Aβ+ CI group with those of the preclinical AD group also revealed a cluster of hypoconnectivity in the symptomatic group. This cluster consisted of 11 connections, 9 of which represented either PRC- or ERC-associated connectivity (Fig. 3d).

Taken together, the above results suggest that the PRC (and possibly ERC) connectivity follows an inverse 'U-shaped' pattern that is characterized by an initial rise during the preclinical phase and a decline during the symptomatic stage. To verify this effect, we computed mean connectivity scores for the right PRC connections that displayed hyperconnectivity in the preclinical vs. control comparison above and examined how those PRC connectivity profiles differed at various stages of the AD continuum. Group comparisons [two-way ANCOVAs; Group and Sex as fixed factors; Age and Head Movement metrics as covariates] of these overall PRC connectivity measures showed that intra-MTL PRC connectivity was higher in the Aβ+ CU group than in the other two groups [Aβ+ CU vs. Aβ− CU comparison: $F_{1,91} = 25.90$, Holm-Bonferroni-corrected $p < 0.001$; Aβ+ CI vs. Aβ+ CU comparison: $F_{1,54} = 25.89$, Holm-Bonferroni-corrected $p < 0.001$]. However, right PRC connectivity of the Aβ− CU group did not differ from that of the Aβ+ CI group (uncorrected $p = 0.95$). Thus, our results indicate excess functional synchronicity in the anterior MTL only during the asymptomatic stage of the disease [age-, gender-, and motion-corrected PRC connectivity means in Fisher's *Z*-score units: $M_{A\beta- CU} = 0.085$, $M_{A\beta+ CU} = 0.209$, $M_{A\beta+ CI} = 0.085$; Fig. 3f].

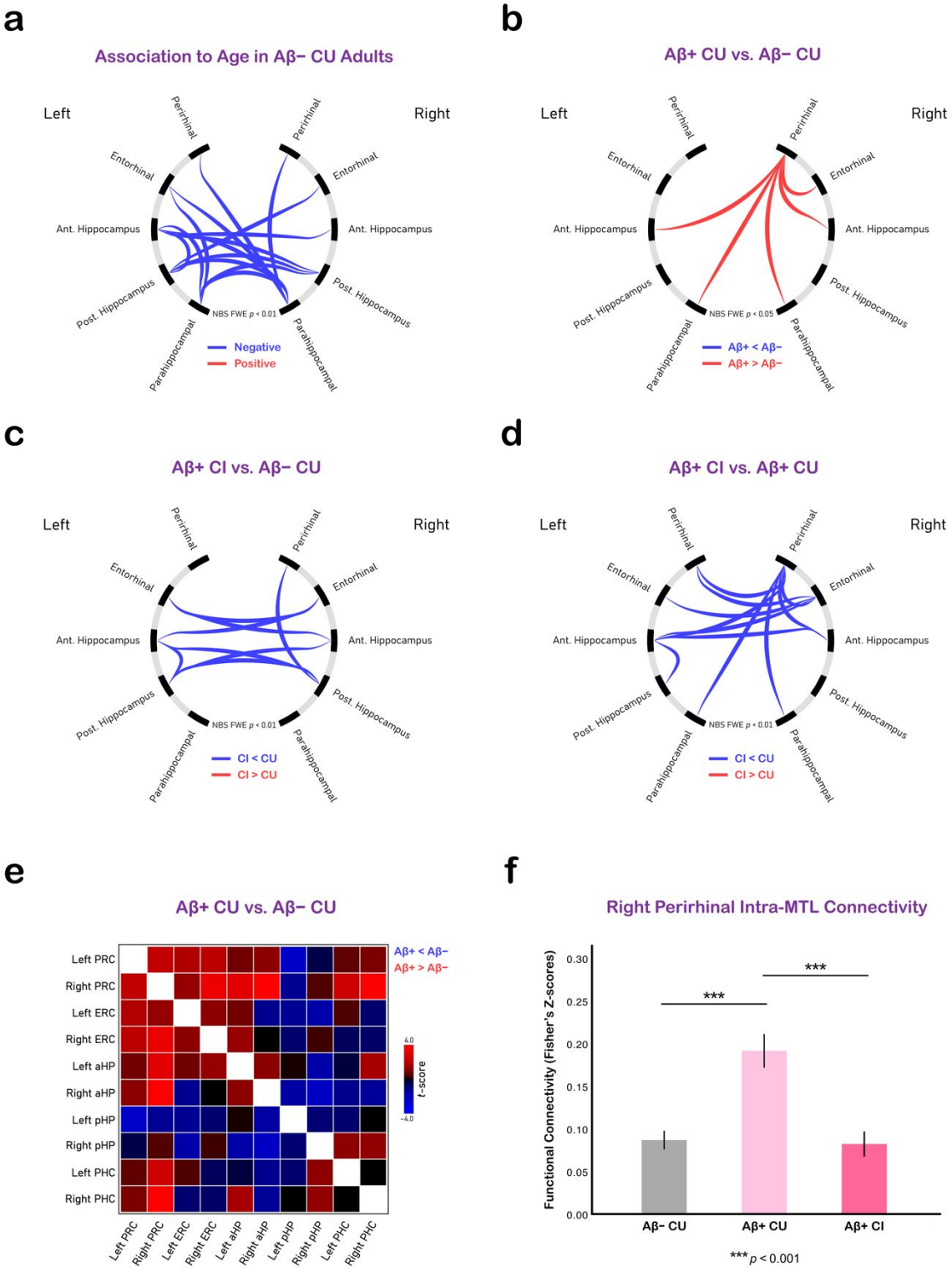

Figure 3. Connectograms representing the effects of **(a)** age and **(b-d)** AD progression on intra-MTL functional connectivity. **(e)** Matrix-form representation of intra-MTL functional connectivity differences between Aβ-positive individuals with preclinical AD and Aβ-negative age-matched controls. **(f)** Right PRC functional connectivity differences between age-matched Aβ-negative normal agers, Aβ-positive cognitively normal individuals with preclinical AD, and Aβ-positive individuals with symptomatic disease. Abbreviations: PRC = perirhinal cortex; ERC = entorhinal cortex; PHC = parahippocampal cortex; aHP = anterior hippocampus; pHP = posterior hippocampus; CU = cognitively unimpaired; CI, cognitively impaired; NBS = network-based statistic.

In summary, our intra-MTL connectivity comparisons revealed PRC hyperconnectivity in cognitively normal amyloid-positive individuals and HP hypoconnectivity in patients with symptomatic disease. In normal agers, we observed age-associated FC decline that was centered around the PHC connections. Furthermore, these trends did not change if partial correlations were used to model intra-MTL functional interactions (Suppl. Fig. 2).

The Effects of Age and AD Progression on the AT and PM Networks

Both network systems displayed declining intra-network FC as a function of age, while no positive relationships to age were detected in either system (Fig. 4a). Relationships to age within the AT and PM systems were represented by single 20-edge and 40-edge clusters, respectively. Only the AT network's cluster contained an edge with a direct link to one of the tau-based MTL ROIs (Fig. 4a). In analyses of AT-PM inter-network FC only the $aMTL_{tau}$-$pMTL_{tau}$ edge in the left hemisphere had a statistically significant negative relationship to age (Suppl. Fig. 3), demonstrating that FC between the anterior and posterior MTL segments declines with age. We did not observe any statistically significant positive relationships between age and AT-PM inter-module FC.

Consistent with the intra-MTL effects detailed above, the preclinical AD group displayed AT-specific hyperconnectivity relative to age-matched amyloid-negative controls. This excess connectivity was represented by a single cluster of connections, all but one of which emanated from the $aMTL_{tau}$ ROIs. As in the intra-MTL results, the AT-specific hyperconnectivity was more prominent in the right hemisphere and was not present in the symptomatic group (Fig. 4b). No FC differences between Aβ− CU and the Aβ+ CU groups were detected in the PM system (Fig. 4b). Relative to normal agers, patients with MCI and prodromal AD displayed reduced FC within the PM, but not the AT, system (Fig. 4c). Furthermore, in congruence with our intra-MTL findings, our analyses of the AT and PM networks indicate that hyperconnectivity within the AT system declines as pathology and symptoms progress beyond the preclinical stage (Fig. 4d). No

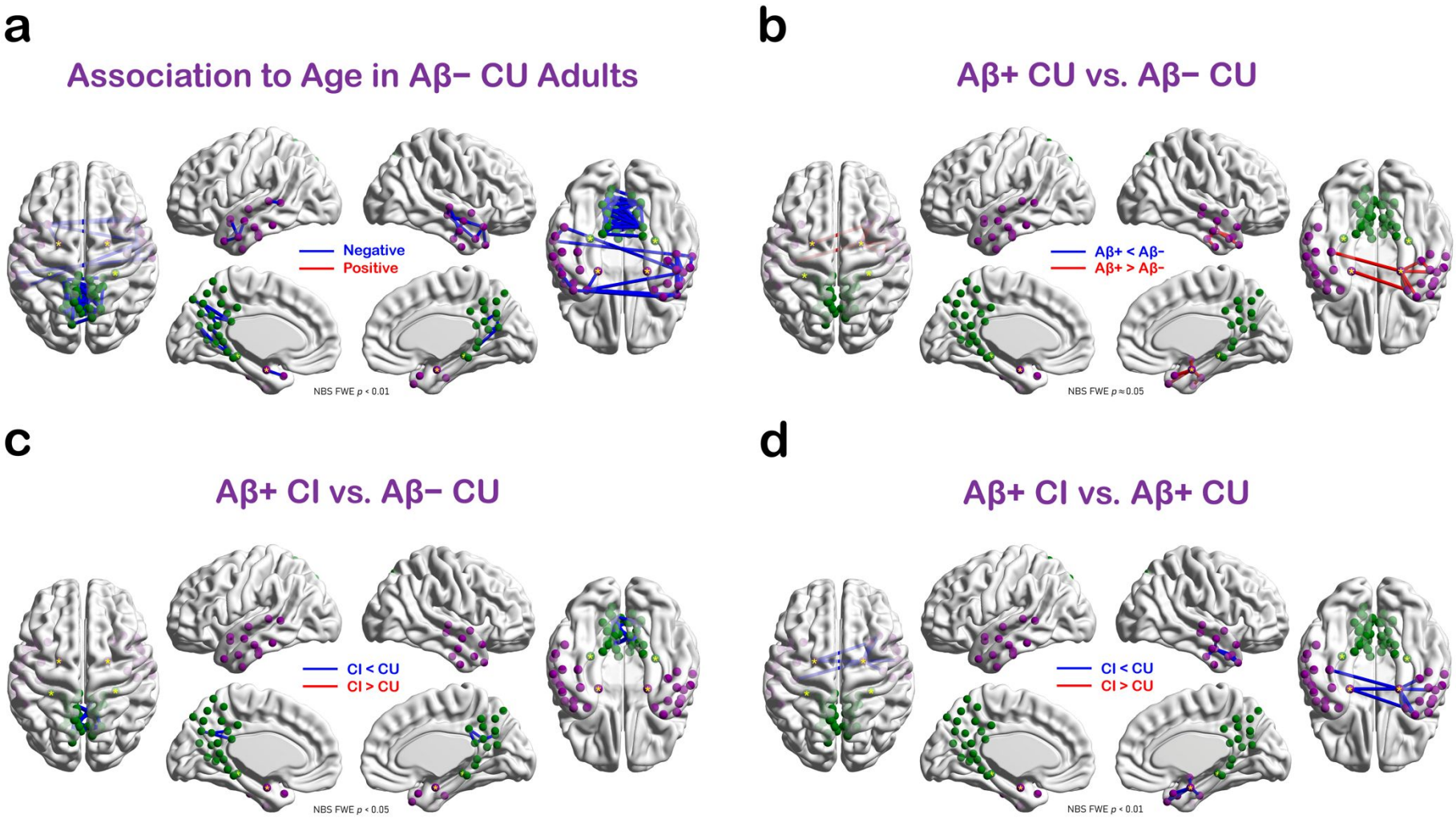

Figure 4. Effects of **(a)** age and **(b-d)** AD progression on intra-network connectivity of the AT and PM systems. AT nodes are in purple; PM nodes are in green. Tau-based MTL ROIs are marked with a yellow asterisk. Abbreviations: AT = anterior-temporal; PM = posterior-medial; CU = cognitively unimpaired; CI, cognitively impaired.

differences in the AT-PM inter-network FC were found between the Aβ− CU, Aβ+ CU, and Aβ+ CI groups.

In order to further examine the effects of age on those connections that link the $aMTL_{tau}$ and $pMTL_{tau}$ ROIs to their respective networks, we first computed average functional connectivity scores of all such connections (i.e., one-hop $aMTL_{tau}$-AT and $pMTL_{tau}$-PM connectivity; Figs. 5-6). In normal agers, both the $aMTL_{tau}$-AT and $pMTL_{tau}$-PM one-hop FC was negatively associated with age (Fig. 5). Next, we evaluated the effect of disease progression on the $aMTL_{tau}$-AT and $pMTL_{tau}$-PM connectivity (Fig. 6). Disease stage group differences were statistically significant for the $aMTL_{tau}$-AT connections ($F_{2,131} = 9.17$, $p < 0.001$), and showed a trend towards statistical significance for the $pMTL_{tau}$-PM connections ($F_{2,131} = 2.68$, $p = 0.072$). Follow-up pairwise comparisons revealed that the $aMTL_{tau}$-AT FC was greater in the Aβ+ CU group relative to the Aβ− CU control group [$F_{1,131} = 11.98$, Holm-Bonferroni-corrected FWE $p = 0.001$, $M_{diff} = 0.084$ Fisher's Z-score units; Fig. 6] and relative to the Aβ+ CI patient group [$F_{1,131} = 17.76$; Holm-Bonferroni-corrected $p < 0.001$, $M_{diff} = 0.114$ Fisher's Z-score units; Fig. 6]. No statistical differences in the $aMTL_{tau}$-AT connectivity were observed between the Aβ− CU and Aβ+ CI groups (uncorrected $p = 0.148$; Fig. 6). For the $pMTL_{tau}$-PM analyses, we did not find an increase in Aβ+ CI connectivity relative to the other groups. However, we observed a trend towards lower connectivity in the Aβ+ CI group relative to the Aβ− CU group [$F_{1,131} = 5.16$, Holm-Bonferroni-corrected FWE $p = 0.074$; Fig. 6].

In summary, intra-network FC of both network systems displayed a progressive decline with age in Aβ-negative CU adults. The preclinical stage of AD, on the other hand, was characterized by increased functional synchronicity within the AT system, driven mainly by the $aMTL_{tau}$-AT one-hop connections. Lastly, our results revealed that Aβ-positive individuals in the early stages of symptomatic AD displayed hypoconnectivity within the PM network.

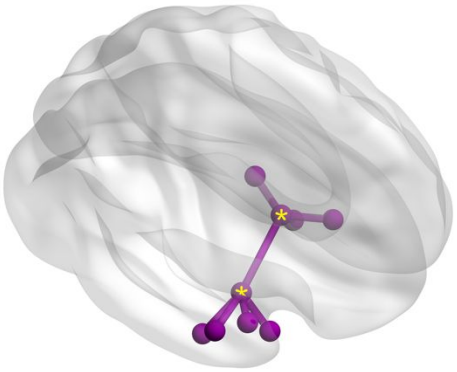

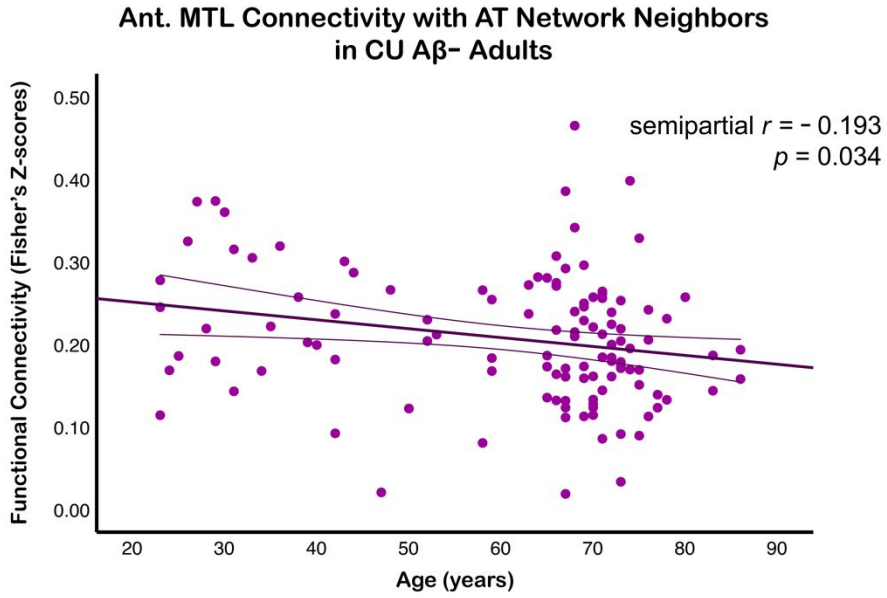

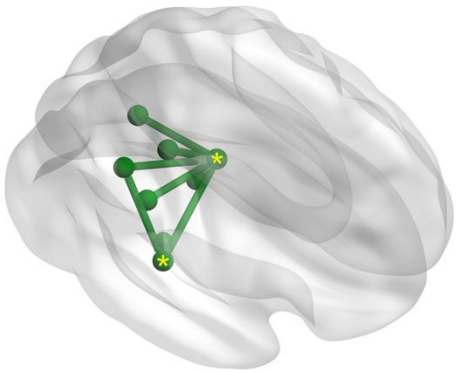

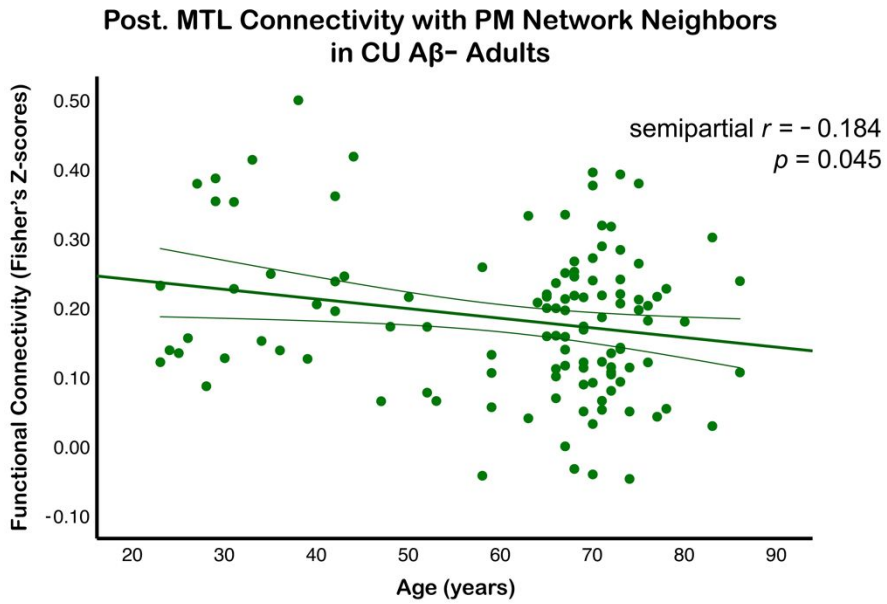

Figure 5. Age relationships for $aMTL_{tau}$-AT and $pMTL_{tau}$-PM functional connectivity. The $aMTL_{tau}$-AT/$pMTL_{tau}$-PM connectivity metric was computed by averaging connectivity values of those edges that represented direct functional interactions between the $aMTL_{tau}$ (or $pMTL_{tau}$) ROIs and their one-hop neighbors in the AT (or PM) network (top and bottom glass brains, respectively). Lifespan trajectories are surrounded by thin lines that represent 95% confidence intervals. The AT network's nodes and edges are shown in purple; those of the PM network are shown in green. Tau-based MTL ROIs are marked with a yellow asterisk. Abbreviations: AT = anterior-temporal; PM = posterior-medial; MTL = medial temporal lobe; $aMTL_{tau}$ = tau-based anterior MTL ROI; $pMTL_{tau}$ = tau-based posterior MTL ROI; CU = cognitively unimpaired; Ant. = anterior; Post. = posterior.

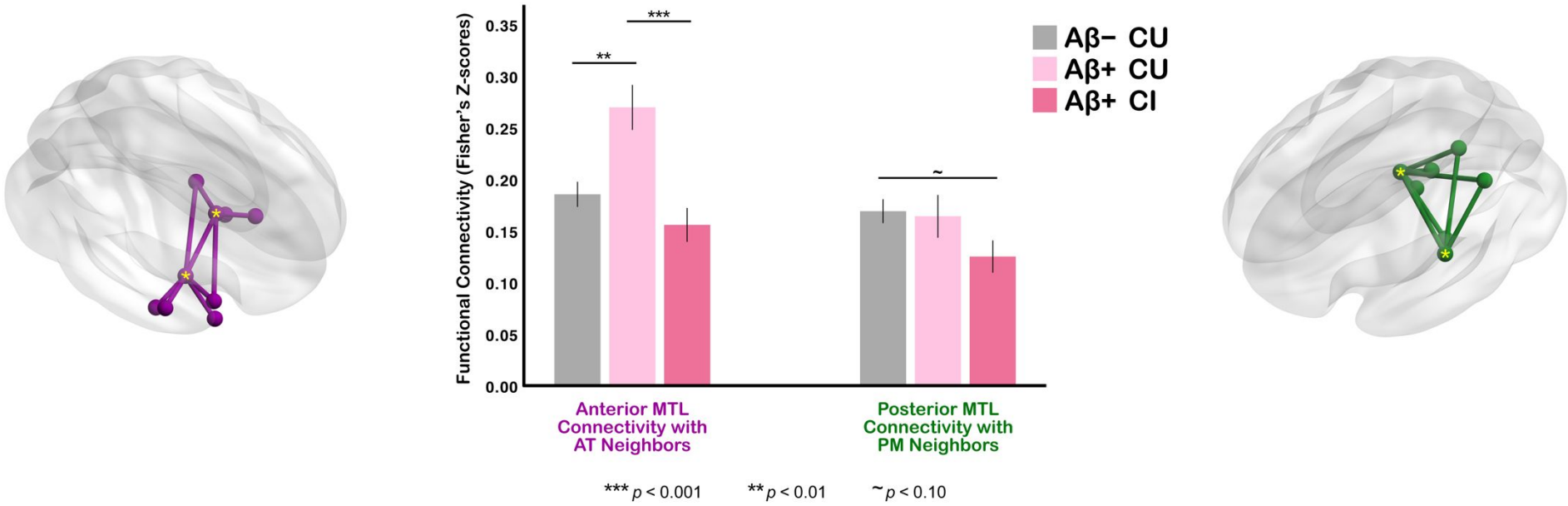

Figure 6. Effect of AD progression on $aMTL_{tau}$-AT and $pMTL_{tau}$-PM functional connectivity. The bar plot depicts statistical differences in the $aMTL_{tau}$-AT and $pMTL_{tau}$-PM connectivity between Aβ-negative cognitively unimpaired older adults, Aβ-positive cognitively unimpaired individuals with preclinical AD, and Aβ-positive individuals with symptomatic disease. The $aMTL_{tau}$-AT connections that were used in these group comparisons are shown to the left of the bar plot; the $pMTL_{tau}$-PM connections are shown to its right. The AT network's nodes and edges are in purple; those of the PM network are in green. Tau-based MTL ROIs are marked with a yellow asterisk. Abbreviations: AT = anterior-temporal; PM = posterior-medial; MTL = medial temporal lobe; $aMTL_{tau}$ = tau-based anterior MTL ROI; $pMTL_{tau}$ = tau-based posterior MTL ROI; CU = cognitively unimpaired; CI = cognitively impaired.

DISCUSSION

We conducted a detailed investigation of MTL FC changes in normal aging and preclinical and symptomatic AD. We paid particular attention to the anterior-posterior axis of the MTL to determine whether the anterior or posterior MTL segments were more vulnerable to age- or AD-related network dysfunction. Our most intriguing finding is the inverse 'U-shaped' FC pattern in the anterior MTL from normal aging to preclinical AD to symptomatic AD. The preclinical stage of AD was characterized by excessive FC centered around areas of the anterior MTL that are prone to early tauopathy. In patients with symptomatic disease, hyperconnectivity was no longer present. Instead, we observed reduced connectivity within the PM system and between various segments of the hippocampus. In contrast to the hyperconnectivity seen in preclinical AD, advanced age was associated with reduced intra-network FC in both the AT and PM systems. Within the MTL, we observed greater vulnerability of the posterior MTL, especially the PHC connections, to age-associated connectivity decline. Together, our results indicate that MTL network dysfunction in AD is not simply an accelerated form of normal aging.

Hyperconnectivity in the Anterior Medial Temporal Lobe in Preclinical AD

In our earlier work, we reported increased FC between the ERC and other regions of the MTL in amnesic MCI.[43] Later studies by others confirmed those findings.[22,45] However, it was not obvious how early in the course of AD this effect first appears, and conflicting results have been published on the nature of the MTL network disruption at more advanced stages.[45,114] Our results demonstrated that the anterior MTL hyperconnectivity is present in individuals with preclinical but not prodromal AD. Inverse 'U-shaped' FC patterns of this type have been previously identified in the default mode and salience networks.[115] To our knowledge, only one other study reported elevated FC levels in the AT network among older individuals with memory complaints but not in patients with dementia due to AD.[114] However, that study did not use PET or CSF biomarkers to screen for preclinical AD, and because of resolution limitations, it had limited anatomical specificity within the MTL.

The physiology underlying network hyperconnectivity in preclinical AD is unknown. Epidemiological studies indicate an elevated prevalence of subclinical seizures in both early-onset and late-onset AD,[116-118] frequently originating in the temporal cortex and associated with earlier onset of cognitive symptoms.[119] Even though we did not observe any differences in cognitive capacity between normal agers and CU participants with preclinical AD, it is plausible that increased anterior MTL connectivity in this group represents circuit dysfunction as opposed to compensatory processes. For instance, Bakker *et al.*[120] showed that administering a low dose of the anti-epileptic drug levetiracetam to patients with amnesic MCI can result in memory improvement.

To our best knowledge, only a single human imaging study by Berron *et al.*[22] examined the effects of preclinical and symptomatic AD on both the AT and PM networks. They reported decreased FC between the medial prefrontal cortex and the ERC/PRC region of the MTL in preclinical AD and decreased MTL-PM FC in Aβ+ individuals with amnesic MCI. Thus, it is plausible that functional abnormalities in preclinical AD are characterized not only by local and regional $aMTL_{tau}$ hyperconnectivity but also by reduced connectivity between the anterior MTL and more distant regions of the neocortex. Furthermore, according to our current results, the MTL subregions most likely to show NFT accumulation are also the ones to display patterns of excessive connectivity in early stages of AD. Harrison *et al.*[121] reached a similar conclusion for intra-HP connectivity, demonstrating a positive relationship between the intra-HP signal coherence (a measure of local connectivity) and tau burden in the ERC among CU older adults.

Animal and *in vitro* research has revealed that hyperactivity within the MTL enhances both amyloid and tau pathology in the HP and ERC,[48,53-55,122,123] while the earliest stages of neuronal dysfunction in AD mice are characterized by Aβ-induced hyperactivity with hypoactivation appearing in later stages of the disease.[124] Using mice models of AD, Angulo *et al.*[49] studied the effects of Aβ and tau on ERC neurons specifically. Consistent with findings from non-ERC MTL subregions, Aβ – in the absence of tau – induced hyperexcitability in the ERC circuits; however, co-expression of both Aβ and tau moderated the excitatory effects of Aβ on the ERC.[49] This is

broadly consistent with our findings of increased connectivity in the anterior MTL only during the preclinical stage of AD when tau levels are expected to be low. Alternatively, by symptomatic stages of the disease, most individuals are expected to have a more significant tau burden both within the MTL and beyond.[12,16,55,125-128]

In this context, our results support the hypothesis that the earliest pathological processes in AD result in MTL network dysfunction centered around the anterior MTL subregions, possibly caused by Aβ-induced hyperexcitability. Such elevated activity levels likely accelerate NFT formation and spread, leading to synapse loss and network breakdown over time.

Intra-MTL Functional Connectivity Changes in Normal Aging

We showed that posterior MTL subregions, and especially the PHC, become increasingly decoupled from the rest of the MTL with age. On standardized psychological assessments, older adults attain lower scores on tests of recollection and relational/associative memory, while familiarity-based item recognition is largely unaffected by age.[67-71,129] Declining performance on tests of associative/relational memory indicates posterior, as opposed to anterior, MTL dysfunction in older adults.[6,7,130] Consistent with the evidence from cognitive work, Panitz *et al.*[131] reported reduced intra-HP connectivity in older participants, but only in the middle-posterior HP segments. Similarly, some structural MRI studies reported greater vulnerability of the posterior MTL subregions to atrophy in normal aging.[18,132-134]

In a task-based study of intra-MTL FC, Stark *et al.*[135] compared PRC-HP, ERC-HP, and PHC-HP connectivity profiles of CU young (< 40 years) and CU old (≥ 70 years) adults. The authors reported reduced aHP-PHC connectivity among the elderly and a smaller but also significant reduction of the PRC-HP FC. However, group differences were not found in the more anterior ERC-HP connections. In the rs-fMRI literature, the effects of age on HP- and PHC-associated FC have been examined by Damoiseaux *et al.,*[136] who reported negative age relationships for the anterior-posterior and interhemispheric intra-HP connections. By focusing on spontaneous

network dynamics at rest and by studying all memory-related MTL subregions, not just the HP and PHC, we advanced the understanding about the effects of normal aging on intra-MTL FC.

Effects of Age on Functional Connectivity Properties of the AT and PM Networks

This is the first FC study to document age-related alterations in the AT and PM intra- and inter-network connectivity for the entire adult lifespan. Initial imaging evidence for altered network dynamics in old age was demonstrated in task-based fMRI and PET experiments, which showed an over-recruitment of frontal and parietal association cortices in older cohorts relative to younger cohorts across a wide variety of cognitive tasks.[137-147] Studies of spontaneous BOLD signal fluctuations also found a negative relationship between age and network specialization across standard cerebral networks, which often manifests as increased inter-network connectivity in older participants.[66,148-154] Contrary to these observations, we did not detect any positive relationships between age and AT-PM inter-network connectivity. Instead, our results indicate reduced AT-PM interactions in older adults. This lack of agreement with earlier literature might be a consequence of our exclusive focus on the AT-PM connections. It is still plausible that the AT and PM networks undergo age-related despecialization, just not in their interactions with each other. Alternatively, MTL-affiliated network systems might be more resilient to the age-associated loss of functional specialization than other brain systems. Contrary to the inter-network results, our present findings on the AT and PM intra-network connectivity are broadly consistent with the aging literature from other groups, which also reported reduced intra-network interactions in cognitively normal older adults.[60,63-66,155,156]

Limitations and Future Work

A few caveats merit discussion. First, as is the case with most fMRI studies of the MTL, the anterior MTL subregions in our study were more vulnerable to susceptibility artifacts from the skull base than their posterior counterparts. However, because both raw and preprocessed temporal signal-to-noise ratio (tSNR) profiles for each ASHS-T1 ROI were similar across groups

(Suppl. Table 1), it is unlikely that susceptibility effects biased our main findings. Second, because of acquisition constraints, we assumed a common network architecture for all participants in a given statistical comparison. Despite high levels of structural consistency, inter-individual variability in network architecture exists,[157-159] and exploring individual differences in the AT and PM network profiles at different stages of AD progression is a valuable avenue for future research.

Head motion has been shown to modulate FC in multiple brain networks.[160-162] As in other studies involving older adults,[64,163] head movement in our current study was correlated with age. Our preprocessing pipeline was designed with this issue in mind. Furthermore, among the three older groups [i.e., CU Aβ-, CU Aβ+, CI Aβ+] the amount of head motion was similar (Suppl. Table 2). Consequently, it is unlikely that our main findings were driven by head movement artifacts.

Conceptually, the present study focused only on the anterior-posterior axis of the MTL; however, work by others demonstrated functional specialization and differential AD pathology within the medial-to-lateral axis as well.[10,20,36,135,164-167] Future studies employing high-field high-resolution fMRI acquisitions will be able to study the effects of AD progression on both axes simultaneously.

Although we infer opposite effects of Aβ and tau NFT on anterior MTL connectivity from our results, the proposed model needs further validation on participants who underwent both amyloid-PET and tau-PET scans. Lastly, the cross-sectional nature of our design – and all limitations that accompany cross-sectional studies of aging and AD – need to be acknowledged.

CONCLUSION

Our results suggest that MTL-AT connectivity follows an inverse 'U-shaped' pattern in AD. The earliest phase of AD is characterized by elevated MTL-AT connectivity. This effect originates from the MTL regions that are most susceptible to early tauopathy. As the disease progresses, MTL-AT connectivity declines and hypoconnectivity appears in the PM network. In normal aging, both the AT and PM networks displayed intra-network connectivity decline; however, the deleterious effects of age were more pronounced in the posterior MTL subregions. Thus, MTL functional connectivity is a dynamic process in normal aging and in AD.

FUNDING

The work in the present study was supported by the Alzheimer's Association Grant AARF-21-848972 and by the National Institutes of Health Grants P30-AG072979, RF1-AG069474, R01-AG056014, R01-AG055005, R01-AG072796 and R01-AG070592.

COMPETING INTERESTS

D.A.W. has served as a paid consultant to Eli Lilly, GE Healthcare, and Qynapse. He serves on a DSMB for Functional Neuromodulation. He receives research support paid to his institution from Biogen. I.N. serves on the Scientific Advisory Board for Eisai and does educational speaking for Biogen. All other authors report no competing interests.

REFERENCES

1. Cohen NJ, Ryan J, Hunt C, Romine L, Wszalek T, Nash C. Hippocampal system and declarative (relational) memory: summarizing the data from functional neuroimaging studies. *Hippocampus*. 1999;9(1):83-98. doi:10.1002/(SICI)1098-1063(1999)9:1<83::AID-HIPO9>3.0.CO;2-7

2. Hrybouski S, Aghamohammadi-Sereshki A, Madan CR*, et al*. Amygdala subnuclei response and connectivity during emotional processing. *Neuroimage*. Jun 2016;133:98-110. doi:10.1016/j.neuroimage.2016.02.056

3. Kensinger EA. Remembering the Details: Effects of Emotion. *Emot Rev*. 2009;1(2):99-113. doi:10.1177/1754073908100432

4. Lisman J, Buzsaki G, Eichenbaum H, Nadel L, Ranganath C, Redish AD. Viewpoints: how the hippocampus contributes to memory, navigation and cognition. *Nat Neurosci*. Oct 26 2017;20(11):1434-1447. doi:10.1038/nn.4661

5. Moscovitch M, Cabeza R, Winocur G, Nadel L. Episodic Memory and Beyond: The Hippocampus and Neocortex in Transformation. *Annu Rev Psychol*. 2016;67:105-34. doi:10.1146/annurev-psych-113011-143733

6. Ranganath C, Ritchey M. Two cortical systems for memory-guided behaviour. *Nat Rev Neurosci*. Oct 2012;13(10):713-26. doi:10.1038/nrn3338

7. Poppenk J, Evensmoen HR, Moscovitch M, Nadel L. Long-axis specialization of the human hippocampus. *Trends Cogn Sci*. May 2013;17(5):230-40. doi:10.1016/j.tics.2013.03.005

8. Squire LR, Genzel L, Wixted JT, Morris RG. Memory consolidation. *Cold Spring Harb Perspect Biol*. Aug 3 2015;7(8):a021766. doi:10.1101/cshperspect.a021766

9. Jeneson A, Squire LR. Working memory, long-term memory, and medial temporal lobe function. *Learn Mem*. Jan 2012;19(1):15-25. doi:10.1101/lm.024018.111

10. Hrybouski S, MacGillivray M, Huang Y*, et al*. Involvement of hippocampal subfields and anterior-posterior subregions in encoding and retrieval of item, spatial, and associative memories: Longitudinal versus transverse axis. *Neuroimage*. May 1 2019;191:568-586. doi:10.1016/j.neuroimage.2019.01.061

11. Jagust W. Imaging the evolution and pathophysiology of Alzheimer disease. *Nat Rev Neurosci*. Nov 2018;19(11):687-700. doi:10.1038/s41583-018-0067-3

12. Small SA, Swanson LW. A Network Explanation of Alzheimer's Regional Vulnerability. *Cold Spring Harb Symp Quant Biol*. 2018;83:193-200. doi:10.1101/sqb.2018.83.036889

13. Small SA, Schobel SA, Buxton RB, Witter MP, Barnes CA. A pathophysiological framework of hippocampal dysfunction in ageing and disease. *Nat Rev Neurosci*. Sep 7 2011;12(10):585-601. doi:10.1038/nrn3085

14. Yassa MA. Ground zero in Alzheimer's disease. *Nat Neurosci*. Feb 2014;17(2):146-7. doi:10.1038/nn.3631

15. Genon S, Bernhardt BC, La Joie R, Amunts K, Eickhoff SB. The many dimensions of human hippocampal organization and (dys)function. *Trends Neurosci*. Dec 2021;44(12):977-989. doi:10.1016/j.tins.2021.10.003

16. Braak H, Alafuzoff I, Arzberger T, Kretzschmar H, Del Tredici K. Staging of Alzheimer disease-associated neurofibrillary pathology using paraffin sections and immunocytochemistry. *Acta Neuropathol*. Oct 2006;112(4):389-404. doi:10.1007/s00401-006-0127-z

17. Braak H, Braak E. Neuropathological stageing of Alzheimer-related changes. *Acta Neuropathol*. 1991;82(4):239-59. doi:10.1007/BF00308809

18. Malykhin NV, Huang Y, Hrybouski S, Olsen F. Differential vulnerability of hippocampal subfields and anteroposterior hippocampal subregions in healthy cognitive aging. *Neurobiol Aging*. Nov 2017;59:121-134. doi:10.1016/j.neurobiolaging.2017.08.001

19. Xie L, Wisse LEM, Das SR*, et al*. Longitudinal atrophy in early Braak regions in preclinical Alzheimer's disease. *Hum Brain Mapp*. Nov 2020;41(16):4704-4717. doi:10.1002/hbm.25151

20. Yushkevich PA, Munoz Lopez M, Iniguez de Onzono Martin MM*, et al*. Three-dimensional mapping of neurofibrillary tangle burden in the human medial temporal lobe. *Brain*. Oct 22 2021;144(9):2784-2797. doi:10.1093/brain/awab262

21. Bota M, Sporns O, Swanson LW. Architecture of the cerebral cortical association connectome underlying cognition. *Proc Natl Acad Sci U S A*. Apr 21 2015;112(16):E2093-101. doi:10.1073/pnas.1504394112

22. Berron D, van Westen D, Ossenkoppele R, Strandberg O, Hansson O. Medial temporal lobe connectivity and its associations with cognition in early Alzheimer's disease. *Brain*. Apr 1 2020;143(4):1233-1248. doi:10.1093/brain/awaa068

23. Das SR, Pluta J, Mancuso L, Kliot D, Yushkevich PA, Wolk DA. Anterior and posterior MTL networks in aging and MCI. *Neurobiol Aging*. Jan 2015;36 Suppl 1:S141-50, S150 e1. doi:10.1016/j.neurobiolaging.2014.03.041

24. de Flores R, Das SR, Xie L*, et al*. Medial Temporal Lobe Networks in Alzheimer's Disease: Structural and Molecular Vulnerabilities. *J Neurosci*. Mar 9 2022;42(10):2131-2141. doi:10.1523/JNEUROSCI.0949-21.2021

25. Libby LA, Ekstrom AD, Ragland JD, Ranganath C. Differential connectivity of perirhinal and parahippocampal cortices within human hippocampal subregions revealed by high-resolution functional imaging. *J Neurosci*. May 9 2012;32(19):6550-60. doi:10.1523/JNEUROSCI.3711-11.2012

26. Maass A, Berron D, Libby LA, Ranganath C, Duzel E. Functional subregions of the human entorhinal cortex. *Elife*. Jun 8 2015;4doi:10.7554/eLife.06426

27. Maass A, Berron D, Harrison TM*, et al*. Alzheimer's pathology targets distinct memory networks in the ageing brain. *Brain*. Aug 1 2019;142(8):2492-2509. doi:10.1093/brain/awz154

28. Targa Dias Anastacio H, Matosin N, Ooi L. Neuronal hyperexcitability in Alzheimer's disease: what are the drivers behind this aberrant phenotype? *Transl Psychiatry*. Jun 22 2022;12(1):257. doi:10.1038/s41398-022-02024-7

29. Mucke L, Selkoe DJ. Neurotoxicity of amyloid beta-protein: synaptic and network dysfunction. *Cold Spring Harb Perspect Med*. Jul 2012;2(7):a006338. doi:10.1101/cshperspect.a006338

30. Palop JJ, Mucke L. Network abnormalities and interneuron dysfunction in Alzheimer disease. *Nat Rev Neurosci*. Dec 2016;17(12):777-792. doi:10.1038/nrn.2016.141

31. Sperling R, Mormino E, Johnson K. The evolution of preclinical Alzheimer's disease: implications for prevention trials. *Neuron*. Nov 5 2014;84(3):608-22. doi:10.1016/j.neuron.2014.10.038

32. Johnson SC, Baxter LC, Susskind-Wilder L, Connor DJ, Sabbagh MN, Caselli RJ. Hippocampal adaptation to face repetition in healthy elderly and mild cognitive impairment. *Neuropsychologia*. 2004;42(7):980-9. doi:10.1016/j.neuropsychologia.2003.11.015

33. Hämäläinen A, Pihlajamäki M, Tanila H*, et al*. Increased fMRI responses during encoding in mild cognitive impairment. *Neurobiol Aging*. Dec 2007;28(12):1889-903. doi:10.1016/j.neurobiolaging.2006.08.008

34. Kircher TT, Weis S, Freymann K*, et al*. Hippocampal activation in patients with mild cognitive impairment is necessary for successful memory encoding. *J Neurol Neurosurg Psychiatry*. Aug 2007;78(8):812-8. doi:10.1136/jnnp.2006.104877

35. Huijbers W, Mormino EC, Schultz AP*, et al*. Amyloid-beta deposition in mild cognitive impairment is associated with increased hippocampal activity, atrophy and clinical progression. *Brain*. Apr 2015;138(Pt 4):1023-35. doi:10.1093/brain/awv007

36. Yassa MA, Stark SM, Bakker A, Albert MS, Gallagher M, Stark CE. High-resolution structural and functional MRI of hippocampal CA3 and dentate gyrus in patients with amnestic Mild Cognitive Impairment. *Neuroimage*. Jul 1 2010;51(3):1242-52. doi:10.1016/j.neuroimage.2010.03.040

37. Bookheimer SY, Strojwas MH, Cohen MS*, et al*. Patterns of brain activation in people at risk for Alzheimer's disease. *N Engl J Med*. Aug 17 2000;343(7):450-6. doi:10.1056/NEJM200008173430701

38. Tran TT, Speck CL, Pisupati A, Gallagher M, Bakker A. Increased hippocampal activation in ApoE-4 carriers and non-carriers with amnestic mild cognitive impairment. *Neuroimage Clin*. 2017;13:237-245. doi:10.1016/j.nicl.2016.12.002

39. Johnson SC, Schmitz TW, Trivedi MA*, et al*. The influence of Alzheimer disease family history and apolipoprotein E epsilon4 on mesial temporal lobe activation. *J Neurosci*. May 31 2006;26(22):6069-76. doi:10.1523/JNEUROSCI.0959-06.2006

40. Filippini N, MacIntosh BJ, Hough MG*, et al*. Distinct patterns of brain activity in young carriers of the APOE-epsilon4 allele. *Proc Natl Acad Sci U S A*. Apr 28 2009;106(17):7209-14. doi:10.1073/pnas.0811879106

41. Quiroz YT, Budson AE, Celone K*, et al*. Hippocampal hyperactivation in presymptomatic familial Alzheimer's disease. *Ann Neurol*. Dec 2010;68(6):865-75. doi:10.1002/ana.22105

42. Reiman EM, Quiroz YT, Fleisher AS*, et al*. Brain imaging and fluid biomarker analysis in young adults at genetic risk for autosomal dominant Alzheimer's disease in the presenilin 1 E280A kindred: a case-control study. *Lancet Neurol*. Dec 2012;11(12):1048-56. doi:10.1016/S1474-4422(12)70228-4

43. Das SR, Pluta J, Mancuso L*, et al*. Increased functional connectivity within medial temporal lobe in mild cognitive impairment. *Hippocampus*. Jan 2013;23(1):1-6. doi:10.1002/hipo.22051

44. Liu J, Zhang X, Yu C*, et al*. Impaired Parahippocampus Connectivity in Mild Cognitive Impairment and Alzheimer's Disease. *J Alzheimers Dis*. 2016;49(4):1051-64. doi:10.3233/JAD-150727

45. Pasquini L, Scherr M, Tahmasian M*, et al*. Link between hippocampus' raised local and eased global intrinsic connectivity in AD. *Alzheimers Dement*. May 2015;11(5):475-84. doi:10.1016/j.jalz.2014.02.007

46. Song Z, Insel PS, Buckley S*, et al*. Brain amyloid-beta burden is associated with disruption of intrinsic functional connectivity within the medial temporal lobe in cognitively normal elderly. *J Neurosci*. Feb 18 2015;35(7):3240-7. doi:10.1523/JNEUROSCI.2092-14.2015

47. Toussaint PJ, Maiz S, Coynel D*, et al*. Characteristics of the default mode functional connectivity in normal ageing and Alzheimer's disease using resting state fMRI with a combined approach of entropy-based and graph theoretical measurements. *Neuroimage*. Nov 1 2014;101:778-86. doi:10.1016/j.neuroimage.2014.08.003

48. Abramov E, Dolev I, Fogel H, Ciccotosto GD, Ruff E, Slutsky I. Amyloid-beta as a positive endogenous regulator of release probability at hippocampal synapses. *Nat Neurosci*. Dec 2009;12(12):1567-76. doi:10.1038/nn.2433

49. Angulo SL, Orman R, Neymotin SA*, et al*. Tau and amyloid-related pathologies in the entorhinal cortex have divergent effects in the hippocampal circuit. *Neurobiol Dis*. Dec 2017;108:261-276. doi:10.1016/j.nbd.2017.08.015

50. Busche MA, Konnerth A. Impairments of neural circuit function in Alzheimer's disease. *Philos Trans R Soc Lond B Biol Sci*. Aug 5 2016;371(1700)doi:10.1098/rstb.2015.0429

51. Fogel H, Frere S, Segev O*, et al*. APP homodimers transduce an amyloid-beta-mediated increase in release probability at excitatory synapses. *Cell Rep*. Jun 12 2014;7(5):1560-1576. doi:10.1016/j.celrep.2014.04.024

52. Palop JJ, Chin J, Roberson ED*, et al*. Aberrant excitatory neuronal activity and compensatory remodeling of inhibitory hippocampal circuits in mouse models of Alzheimer's disease. *Neuron*. Sep 6 2007;55(5):697-711. doi:10.1016/j.neuron.2007.07.025

53. Yamamoto K, Tanei ZI, Hashimoto T*, et al*. Chronic optogenetic activation augments abeta pathology in a mouse model of Alzheimer disease. *Cell Rep*. May 12 2015;11(6):859-865. doi:10.1016/j.celrep.2015.04.017

54. Zott B, Simon MM, Hong W*, et al*. A vicious cycle of beta amyloid-dependent neuronal hyperactivation. *Science*. Aug 9 2019;365(6453):559-565. doi:10.1126/science.aay0198

55. Wu JW, Hussaini SA, Bastille IM*, et al*. Neuronal activity enhances tau propagation and tau pathology in vivo. *Nat Neurosci*. Aug 2016;19(8):1085-92. doi:10.1038/nn.4328

56. Khan UA, Liu L, Provenzano FA*, et al*. Molecular drivers and cortical spread of lateral entorhinal cortex dysfunction in preclinical Alzheimer's disease. *Nat Neurosci*. Feb 2014;17(2):304-11. doi:10.1038/nn.3606

57. Price JL, Ko AI, Wade MJ, Tsou SK, McKeel DW, Morris JC. Neuron Number in the Entorhinal Cortex and CA1 in Preclinical Alzheimer Disease. *Archives of Neurology*. 2001;58(9):1395-1402. doi:10.1001/archneur.58.9.1395

58. Gomez-Isla T, Price JL, McKeel DW, Jr., Morris JC, Growdon JH, Hyman BT. Profound loss of layer II entorhinal cortex neurons occurs in very mild Alzheimer's disease. *J Neurosci*. Jul 15 1996;16(14):4491-500. doi:10.1523/JNEUROSCI.16-14-04491.1996

59. Selkoe DJ. Alzheimer's disease is a synaptic failure. *Science*. Oct 25 2002;298(5594):789-91. doi:10.1126/science.1074069

60. Fjell AM, Sneve MH, Grydeland H*, et al*. Functional connectivity change across multiple cortical networks relates to episodic memory changes in aging. *Neurobiol Aging*. Dec 2015;36(12):3255-3268. doi:10.1016/j.neurobiolaging.2015.08.020

61. McDonough IM, Nolin SA, Visscher KM. 25 years of neurocognitive aging theories: What have we learned? *Front Aging Neurosci*. 2022;14:1002096. doi:10.3389/fnagi.2022.1002096

62. Koen JD, Rugg MD. Neural Dedifferentiation in the Aging Brain. *Trends Cogn Sci*. Jul 2019;23(7):547-559. doi:10.1016/j.tics.2019.04.012

63. Allen EA, Erhardt EB, Damaraju E*, et al*. A baseline for the multivariate comparison of resting-state networks. *Front Syst Neurosci*. 2011;5:2. doi:10.3389/fnsys.2011.00002

64. Hrybouski S, Cribben I, McGonigle J*, et al*. Investigating the effects of healthy cognitive aging on brain functional connectivity using 4.7 T resting-state functional magnetic resonance imaging. *Brain Struct Funct*. May 2021;226(4):1067-1098. doi:10.1007/s00429-021-02226-7

65. Andrews-Hanna JR, Snyder AZ, Vincent JL*, et al*. Disruption of large-scale brain systems in advanced aging. *Neuron*. Dec 6 2007;56(5):924-35. doi:10.1016/j.neuron.2007.10.038

66. Betzel RF, Byrge L, He Y, Goni J, Zuo XN, Sporns O. Changes in structural and functional connectivity among resting-state networks across the human lifespan. *Neuroimage*. Nov 15 2014;102 Pt 2:345-57. doi:10.1016/j.neuroimage.2014.07.067

67. Koen JD, Yonelinas AP. Recollection, not familiarity, decreases in healthy ageing: Converging evidence from four estimation methods. *Memory*. 2016;24(1):75-88. doi:10.1080/09658211.2014.985590

68. Wolk DA, Mancuso L, Kliot D, Arnold SE, Dickerson BC. Familiarity-based memory as an early cognitive marker of preclinical and prodromal AD. *Neuropsychologia*. May 2013;51(6):1094-102. doi:10.1016/j.neuropsychologia.2013.02.014

69. Abadie M, Gavard E, Guillaume F. Verbatim and gist memory in aging. *Psychol Aging*. Dec 2021;36(8):891-901. doi:10.1037/pag0000635

70. Alghamdi SA, Rugg MD. The effect of age on recollection is not moderated by differential estimation methods. *Memory*. 2020/09/13 2020;28(8):1067-1077. doi:10.1080/09658211.2020.1813781

71. Cansino S. Episodic memory decay along the adult lifespan: a review of behavioral and neurophysiological evidence. *Int J Psychophysiol*. Jan 2009;71(1):64-9. doi:10.1016/j.ijpsycho.2008.07.005

72. Weintraub S, Besser L, Dodge HH*, et al*. Version 3 of the Alzheimer Disease Centers' Neuropsychological Test Battery in the Uniform Data Set (UDS). *Alzheimer Dis Assoc Disord*. Jan-Mar 2018;32(1):10-17. doi:10.1097/WAD.0000000000000223

73. Nasreddine ZS, Phillips NA, Bedirian V*, et al*. The Montreal Cognitive Assessment, MoCA: a brief screening tool for mild cognitive impairment. *J Am Geriatr Soc*. Apr 2005;53(4):695-9. doi:10.1111/j.1532-5415.2005.53221.x

74. Esteban O, Markiewicz CJ, Blair RW*, et al*. fMRIPrep: a robust preprocessing pipeline for functional MRI. *Nat Methods*. Jan 2019;16(1):111-116. doi:10.1038/s41592-018-0235-4

75. Jenkinson M, Bannister P, Brady M, Smith S. Improved optimization for the robust and accurate linear registration and motion correction of brain images. *Neuroimage*. Oct 2002;17(2):825-41. doi:10.1016/s1053-8119(02)91132-8

76. Smith SM, Jenkinson M, Woolrich MW*, et al*. Advances in functional and structural MR image analysis and implementation as FSL. *Neuroimage*. 2004;23 Suppl 1:S208-19. doi:10.1016/j.neuroimage.2004.07.051

77. Jezzard P, Balaban RS. Correction for geometric distortion in echo planar images from B0 field variations. *Magn Reson Med*. Jul 1995;34(1):65-73. doi:10.1002/mrm.1910340111

78. Greve DN, Fischl B. Accurate and robust brain image alignment using boundary-based registration. *Neuroimage*. Oct 15 2009;48(1):63-72. doi:10.1016/j.neuroimage.2009.06.060

79. Avants B, Gee JC. Geodesic estimation for large deformation anatomical shape averaging and interpolation. *Neuroimage*. 2004;23 Suppl 1:S139-50. doi:10.1016/j.neuroimage.2004.07.010

80. Avants BB, Epstein CL, Grossman M, Gee JC. Symmetric diffeomorphic image registration with cross-correlation: evaluating automated labeling of elderly and neurodegenerative brain. *Med Image Anal*. Feb 2008;12(1):26-41. doi:10.1016/j.media.2007.06.004

81. Beckmann CF, Smith SM. Probabilistic independent component analysis for functional magnetic resonance imaging. *IEEE Trans Med Imaging*. Feb 2004;23(2):137-52. doi:10.1109/TMI.2003.822821

82. Pruim RHR, Mennes M, van Rooij D, Llera A, Buitelaar JK, Beckmann CF. ICA-AROMA: A robust ICA-based strategy for removing motion artifacts from fMRI data. *Neuroimage*. May 15 2015;112:267-277. doi:10.1016/j.neuroimage.2015.02.064

83. Griffanti L, Douaud G, Bijsterbosch J*, et al*. Hand classification of fMRI ICA noise components. *Neuroimage*. Jul 1 2017;154:188-205. doi:10.1016/j.neuroimage.2016.12.036

84. Griffanti L, Salimi-Khorshidi G, Beckmann CF*, et al*. ICA-based artefact removal and accelerated fMRI acquisition for improved resting state network imaging. *Neuroimage*. Jul 15 2014;95:232-47. doi:10.1016/j.neuroimage.2014.03.034

85. Whitfield-Gabrieli S, Nieto-Castanon A. Conn: a functional connectivity toolbox for correlated and anticorrelated brain networks. *Brain Connect*. 2012;2(3):125-41. doi:10.1089/brain.2012.0073

86. Murphy K, Birn RM, Handwerker DA, Jones TB, Bandettini PA. The impact of global signal regression on resting state correlations: are anti-correlated networks introduced? *Neuroimage*. Feb 1 2009;44(3):893-905. doi:10.1016/j.neuroimage.2008.09.036

87. Saad ZS, Gotts SJ, Murphy K*, et al*. Trouble at rest: how correlation patterns and group differences become distorted after global signal regression. *Brain Connect*. 2012;2(1):25-32. doi:10.1089/brain.2012.0080

88. Weissenbacher A, Kasess C, Gerstl F, Lanzenberger R, Moser E, Windischberger C. Correlations and anticorrelations in resting-state functional connectivity MRI: a quantitative comparison of preprocessing strategies. *Neuroimage*. Oct 1 2009;47(4):1408-16. doi:10.1016/j.neuroimage.2009.05.005

89. Behzadi Y, Restom K, Liau J, Liu TT. A component based noise correction method (CompCor) for BOLD and perfusion based fMRI. *Neuroimage*. Aug 1 2007;37(1):90-101. doi:10.1016/j.neuroimage.2007.04.042

90. Friston KJ, Williams S, Howard R, Frackowiak RS, Turner R. Movement-related effects in fMRI time-series. *Magn Reson Med*. Mar 1996;35(3):346-55. doi:10.1002/mrm.1910350312

91. Gratton C, Dworetsky A, Coalson RS*, et al*. Removal of high frequency contamination from motion estimates in single-band fMRI saves data without biasing functional connectivity. *Neuroimage*. Aug 15 2020;217:116866. doi:10.1016/j.neuroimage.2020.116866

92. Fair DA, Miranda-Dominguez O, Snyder AZ*, et al*. Correction of respiratory artifacts in MRI head motion estimates. *Neuroimage*. Mar 2020;208:116400. doi:10.1016/j.neuroimage.2019.116400

93. Xie L, Wisse LEM, Pluta J*, et al*. Automated segmentation of medial temporal lobe subregions on in vivo T1-weighted MRI in early stages of Alzheimer's disease. *Hum Brain Mapp*. Aug 15 2019;40(12):3431-3451. doi:10.1002/hbm.24607

94. Craddock RC, Jbabdi S, Yan CG*, et al*. Imaging human connectomes at the macroscale. *Nat Methods*. Jun 2013;10(6):524-39. doi:10.1038/nmeth.2482

95. Smith SM, Miller KL, Salimi-Khorshidi G*, et al*. Network modelling methods for FMRI. *Neuroimage*. Jan 15 2011;54(2):875-91. doi:10.1016/j.neuroimage.2010.08.063

96. Liégeois R, Santos A, Matta V, Van De Ville D, Sayed AH. Revisiting correlation-based functional connectivity and its relationship with structural connectivity. *Netw Neurosci*. 2020;4(4):1235-1251. doi:10.1162/netn_a_00166

97. Zalesky A, Fornito A, Bullmore ET. Network-based statistic: identifying differences in brain networks. *Neuroimage*. Dec 2010;53(4):1197-207. doi:10.1016/j.neuroimage.2010.06.041

98. Freedman D, Lane D. A Nonstochastic Interpretation of Reported Significance Levels. *Journal of Business & Economic Statistics*. 1983;1(4):292-298. doi:10.2307/1391660

99. Benjamini Y, Hochberg Y. Controlling the False Discovery Rate: A Practical and Powerful Approach to Multiple Testing. *Journal of the Royal Statistical Society Series B (Methodological)*. 1995;57(1):289-300.

100. Power JD, Mitra A, Laumann TO, Snyder AZ, Schlaggar BL, Petersen SE. Methods to detect, characterize, and remove motion artifact in resting state fMRI. *Neuroimage*. Jan 1 2014;84:320-41. doi:10.1016/j.neuroimage.2013.08.048

101. Malykhin NV, Bouchard TP, Ogilvie CJ, Coupland NJ, Seres P, Camicioli R. Three-dimensional volumetric analysis and reconstruction of amygdala and hippocampal head, body and tail. *Psychiatry Res*. Jul 15 2007;155(2):155-65. doi:10.1016/j.pscychresns.2006.11.011

102. Schaefer A, Kong R, Gordon EM*, et al*. Local-Global Parcellation of the Human Cerebral Cortex from Intrinsic Functional Connectivity MRI. *Cereb Cortex*. Sep 1 2018;28(9):3095-3114. doi:10.1093/cercor/bhx179

103. Friedman J, Hastie T, Tibshirani R. Sparse inverse covariance estimation with the graphical lasso. *Biostatistics*. Jul 2008;9(3):432-41. doi:10.1093/biostatistics/kxm045

104. Fan J, Li R. Variable Selection via Nonconcave Penalized Likelihood and its Oracle Properties. *Journal of the American Statistical Association*. 2001/12/01 2001;96(456):1348-1360. doi:10.1198/016214501753382273

105. Fan J, Feng Y, Wu Y. Network Exploration Via the Adaptive Lasso and Scad Penalties. *Ann Appl Stat*. Jun 1 2009;3(2):521-541. doi:10.1214/08-AOAS215SUPP

106. Zhu Y, Cribben I. Sparse Graphical Models for Functional Connectivity Networks: Best Methods and the Autocorrelation Issue. *Brain Connect*. Apr 2018;8(3):139-165. doi:10.1089/brain.2017.0511

107. Hsieh C-J, Sustik MA, Dhillon IS, Ravikumar P. QUIC: quadratic approximation for sparse inverse covariance estimation. *J Mach Learn Res*. 2014;15:2911-2947.

108. Blondel VD, Guillaume J-L, Lambiotte R, Lefebvre E. Fast unfolding of communities in large networks. *Journal of Statistical Mechanics: Theory and Experiment*. 2008/10/09 2008;2008(10):P10008. doi:10.1088/1742-5468/2008/10/P10008

109. Rubinov M, Sporns O. Weight-conserving characterization of complex functional brain networks. *Neuroimage*. Jun 15 2011;56(4):2068-79. doi:10.1016/j.neuroimage.2011.03.069

110. Sun Y, Danila B, Josić K, Bassler KE. Improved community structure detection using a modified fine-tuning strategy. *Europhysics Letters*. 2009/05/04 2009;86(2):28004. doi:10.1209/0295-5075/86/28004

111. Lancichinetti A, Fortunato S. Consensus clustering in complex networks. *Sci Rep*. 2012;2:336. doi:10.1038/srep00336

112. Rubinov M, Sporns O. Complex network measures of brain connectivity: uses and interpretations. *Neuroimage*. Sep 2010;52(3):1059-69. doi:10.1016/j.neuroimage.2009.10.003

113. Xia M, Wang J, He Y. BrainNet Viewer: a network visualization tool for human brain connectomics. *PLoS One*. 2013;8(7):e68910. doi:10.1371/journal.pone.0068910

114. Gour N, Ranjeva JP, Ceccaldi M*, et al*. Basal functional connectivity within the anterior temporal network is associated with performance on declarative memory tasks. *Neuroimage*. Sep 15 2011;58(2):687-97. doi:10.1016/j.neuroimage.2011.05.090

115. Schultz AP, Chhatwal JP, Hedden T*, et al*. Phases of Hyperconnectivity and Hypoconnectivity in the Default Mode and Salience Networks Track with Amyloid and Tau in Clinically Normal Individuals. *J Neurosci*. Apr 19 2017;37(16):4323-4331. doi:10.1523/JNEUROSCI.3263-16.2017

116. Stargardt A, Swaab DF, Bossers K. Storm before the quiet: neuronal hyperactivity and Abeta in the presymptomatic stages of Alzheimer's disease. *Neurobiol Aging*. Jan 2015;36(1):1-11. doi:10.1016/j.neurobiolaging.2014.08.014

117. Vossel KA, Tartaglia MC, Nygaard HB, Zeman AZ, Miller BL. Epileptic activity in Alzheimer's disease: causes and clinical relevance. *Lancet Neurol*. Apr 2017;16(4):311-322. doi:10.1016/S1474-4422(17)30044-3

118. Kazim SF, Seo JH, Bianchi R*, et al*. Neuronal Network Excitability in Alzheimer's Disease: The Puzzle of Similar versus Divergent Roles of Amyloid beta and Tau. *eNeuro*. Mar-Apr 2021;8(2)doi:10.1523/ENEURO.0418-20.2020

119. Vossel KA, Beagle AJ, Rabinovici GD*, et al*. Seizures and epileptiform activity in the early stages of Alzheimer disease. *JAMA Neurol*. Sep 1 2013;70(9):1158-66. doi:10.1001/jamaneurol.2013.136

120. Bakker A, Krauss GL, Albert MS*, et al*. Reduction of hippocampal hyperactivity improves cognition in amnestic mild cognitive impairment. *Neuron*. May 10 2012;74(3):467-74. doi:10.1016/j.neuron.2012.03.023

121. Harrison TM, Maass A, Adams JN, Du R, Baker SL, Jagust WJ. Tau deposition is associated with functional isolation of the hippocampus in aging. *Nat Commun*. Oct 25 2019;10(1):4900. doi:10.1038/s41467-019-12921-z

122. Busche MA, Eichhoff G, Adelsberger H*, et al*. Clusters of hyperactive neurons near amyloid plaques in a mouse model of Alzheimer's disease. *Science*. Sep 19 2008;321(5896):1686-9. doi:10.1126/science.1162844

123. Pooler AM, Phillips EC, Lau DH, Noble W, Hanger DP. Physiological release of endogenous tau is stimulated by neuronal activity. *EMBO Rep*. Apr 2013;14(4):389-94. doi:10.1038/embor.2013.15

124. Busche MA, Chen X, Henning HA*, et al*. Critical role of soluble amyloid-beta for early hippocampal hyperactivity in a mouse model of Alzheimer's disease. *Proc Natl Acad Sci U S A*. May 29 2012;109(22):8740-5. doi:10.1073/pnas.1206171109

125. Therriault J, Pascoal TA, Lussier FZ*, et al*. Biomarker modeling of Alzheimer's disease using PET-based Braak staging. *Nature Aging*. 2022/06/01 2022;2(6):526-535. doi:10.1038/s43587-022-00204-0

126. Delacourte A, David JP, Sergeant N*, et al*. The biochemical pathway of neurofibrillary degeneration in aging and Alzheimer's disease. *Neurology*. Apr 12 1999;52(6):1158-65. doi:10.1212/wnl.52.6.1158

127. Walker LC, Diamond MI, Duff KE, Hyman BT. Mechanisms of protein seeding in neurodegenerative diseases. *JAMA Neurol*. Mar 1 2013;70(3):304-10. doi:10.1001/jamaneurol.2013.1453

128. Wu JW, Herman M, Liu L*, et al*. Small misfolded Tau species are internalized via bulk endocytosis and anterogradely and retrogradely transported in neurons. *J Biol Chem*. Jan 18 2013;288(3):1856-70. doi:10.1074/jbc.M112.394528

129. Stark SM, Stark CEL. Age-related deficits in the mnemonic similarity task for objects and scenes. *Behav Brain Res*. Aug 30 2017;333:109-117. doi:10.1016/j.bbr.2017.06.049

130. Grady CL. Meta-analytic and functional connectivity evidence from functional magnetic resonance imaging for an anterior to posterior gradient of function along the hippocampal axis. *Hippocampus*. May 2020;30(5):456-471. doi:10.1002/hipo.23164

131. Panitz DY, Berkovich-Ohana A, Mendelsohn A. Age-related functional connectivity along the hippocampal longitudinal axis. *Hippocampus*. Oct 2021;31(10):1115-1127. doi:10.1002/hipo.23377

132. Koenig LN, LaMontagne P, Glasser MF*, et al*. Regional age-related atrophy after screening for preclinical alzheimer disease. *Neurobiol Aging*. Jan 2022;109:43-51. doi:10.1016/j.neurobiolaging.2021.09.010

133. Raz N, Ghisletta P, Rodrigue KM, Kennedy KM, Lindenberger U. Trajectories of brain aging in middle-aged and older adults: regional and individual differences. *Neuroimage*. Jun 2010;51(2):501-11. doi:10.1016/j.neuroimage.2010.03.020

134. Frisoni GB, Ganzola R, Canu E*, et al*. Mapping local hippocampal changes in Alzheimer's disease and normal ageing with MRI at 3 Tesla. *Brain*. Dec 2008;131(Pt 12):3266-76. doi:10.1093/brain/awn280

135. Stark SM, Frithsen A, Stark CEL. Age-related alterations in functional connectivity along the longitudinal axis of the hippocampus and its subfields. *Hippocampus*. Jan 2021;31(1):11-27. doi:10.1002/hipo.23259

136. Damoiseaux JS, Viviano RP, Yuan P, Raz N. Differential effect of age on posterior and anterior hippocampal functional connectivity. *Neuroimage*. Jun 2016;133:468-476. doi:10.1016/j.neuroimage.2016.03.047

137. Cabeza R, Anderson ND, Locantore JK, McIntosh AR. Aging gracefully: compensatory brain activity in high-performing older adults. *Neuroimage*. Nov 2002;17(3):1394-402. doi:10.1006/nimg.2002.1280

138. Grady CL, Maisog JM, Horwitz B*, et al*. Age-related changes in cortical blood flow activation during visual processing of faces and location. *J Neurosci*. Mar 1994;14(3 Pt 2):1450-62.

139. Davis SW, Dennis NA, Daselaar SM, Fleck MS, Cabeza R. Que PASA? The posterior-anterior shift in aging. *Cereb Cortex*. May 2008;18(5):1201-9. doi:10.1093/cercor/bhm155

140. Gutchess AH, Welsh RC, Hedden T*, et al*. Aging and the neural correlates of successful picture encoding: frontal activations compensate for decreased medial-temporal activity. *J Cogn Neurosci*. Jan 2005;17(1):84-96. doi:10.1162/0898929052880048

141. Li HJ, Hou XH, Liu HH, Yue CL, Lu GM, Zuo XN. Putting age-related task activation into large-scale brain networks: A meta-analysis of 114 fMRI studies on healthy aging. *Neurosci Biobehav Rev*. Oct 2015;57:156-74. doi:10.1016/j.neubiorev.2015.08.013

142. Logan JM, Sanders AL, Snyder AZ, Morris JC, Buckner RL. Under-recruitment and nonselective recruitment: dissociable neural mechanisms associated with aging. *Neuron*. Feb 28 2002;33(5):827-40. doi:10.1016/s0896-6273(02)00612-8

143. Rajah MN, D'Esposito M. Region-specific changes in prefrontal function with age: a review of PET and fMRI studies on working and episodic memory. *Brain*. Sep 2005;128(Pt 9):1964-83. doi:10.1093/brain/awh608

144. Schneider-Garces NJ, Gordon BA, Brumback-Peltz CR*, et al*. Span, CRUNCH, and beyond: working memory capacity and the aging brain. *J Cogn Neurosci*. Apr 2010;22(4):655-69. doi:10.1162/jocn.2009.21230

145. Spreng RN, Wojtowicz M, Grady CL. Reliable differences in brain activity between young and old adults: a quantitative meta-analysis across multiple cognitive domains. *Neurosci Biobehav Rev*. Jul 2010;34(8):1178-94. doi:10.1016/j.neubiorev.2010.01.009

146. Sugiura M. Functional neuroimaging of normal aging: Declining brain, adapting brain. *Ageing Res Rev*. Sep 2016;30:61-72. doi:10.1016/j.arr.2016.02.006

147. Grady C. The cognitive neuroscience of ageing. *Nat Rev Neurosci*. Jun 20 2012;13(7):491-505. doi:10.1038/nrn3256

148. Chan MY, Park DC, Savalia NK, Petersen SE, Wig GS. Decreased segregation of brain systems across the healthy adult lifespan. *Proc Natl Acad Sci U S A*. Nov 18 2014;111(46):E4997-5006. doi:10.1073/pnas.1415122111

149. Chong JSX, Ng KK, Tandi J*, et al*. Longitudinal Changes in the Cerebral Cortex Functional Organization of Healthy Elderly. *J Neurosci*. Jul 10 2019;39(28):5534-5550. doi:10.1523/JNEUROSCI.1451-18.2019

150. Geerligs L, Renken RJ, Saliasi E, Maurits NM, Lorist MM. A Brain-Wide Study of Age-Related Changes in Functional Connectivity. *Cereb Cortex*. Jul 2015;25(7):1987-99. doi:10.1093/cercor/bhu012

151. Grady C, Sarraf S, Saverino C, Campbell K. Age differences in the functional interactions among the default, frontoparietal control, and dorsal attention networks. *Neurobiol Aging*. May 2016;41:159-172. doi:10.1016/j.neurobiolaging.2016.02.020

152. Keller JB, Hedden T, Thompson TW, Anteraper SA, Gabrieli JD, Whitfield-Gabrieli S. Resting-state anticorrelations between medial and lateral prefrontal cortex: association with working memory, aging, and individual differences. *Cortex*. Mar 2015;64:271-80. doi:10.1016/j.cortex.2014.12.001

153. Spreng RN, Stevens WD, Viviano JD, Schacter DL. Attenuated anticorrelation between the default and dorsal attention networks with aging: evidence from task and rest. *Neurobiol Aging*. Sep 2016;45:149-160. doi:10.1016/j.neurobiolaging.2016.05.020

154. Vij SG, Nomi JS, Dajani DR, Uddin LQ. Evolution of spatial and temporal features of functional brain networks across the lifespan. *Neuroimage*. Jun 2018;173:498-508. doi:10.1016/j.neuroimage.2018.02.066

155. Damoiseaux JS, Beckmann CF, Arigita EJ*, et al*. Reduced resting-state brain activity in the "default network" in normal aging. *Cereb Cortex*. Aug 2008;18(8):1856-64. doi:10.1093/cercor/bhm207

156. Wu JT, Wu HZ, Yan CG*, et al*. Aging-related changes in the default mode network and its anti-correlated networks: a resting-state fMRI study. *Neurosci Lett*. Oct 17 2011;504(1):62-7. doi:10.1016/j.neulet.2011.08.059

157. Gordon EM, Laumann TO, Adeyemo B, Petersen SE. Individual Variability of the System-Level Organization of the Human Brain. *Cereb Cortex*. Jan 1 2017;27(1):386-399. doi:10.1093/cercor/bhv239

158. Laumann TO, Gordon EM, Adeyemo B*, et al*. Functional System and Areal Organization of a Highly Sampled Individual Human Brain. *Neuron*. Aug 5 2015;87(3):657-70. doi:10.1016/j.neuron.2015.06.037

159. Mueller S, Wang D, Fox MD*, et al*. Individual variability in functional connectivity architecture of the human brain. *Neuron*. Feb 6 2013;77(3):586-95. doi:10.1016/j.neuron.2012.12.028

160. Mowinckel AM, Espeseth T, Westlye LT. Network-specific effects of age and in-scanner subject motion: a resting-state fMRI study of 238 healthy adults. *Neuroimage*. Nov 15 2012;63(3):1364-73. doi:10.1016/j.neuroimage.2012.08.004

161. Power JD, Barnes KA, Snyder AZ, Schlaggar BL, Petersen SE. Spurious but systematic correlations in functional connectivity MRI networks arise from subject motion. *Neuroimage*. Feb 1 2012;59(3):2142-54. doi:10.1016/j.neuroimage.2011.10.018

162. Van Dijk KR, Sabuncu MR, Buckner RL. The influence of head motion on intrinsic functional connectivity MRI. *Neuroimage*. Jan 2 2012;59(1):431-8. doi:10.1016/j.neuroimage.2011.07.044

163. Madan CR. Age differences in head motion and estimates of cortical morphology. *PeerJ*. 2018;6:e5176. doi:10.7717/peerj.5176

164. Das SR, Mechanic-Hamilton D, Pluta J, Korczykowski M, Detre JA, Yushkevich PA. Heterogeneity of functional activation during memory encoding across hippocampal subfields in temporal lobe epilepsy. *Neuroimage*. Oct 15 2011;58(4):1121-30. doi:10.1016/j.neuroimage.2011.06.085

165. Bakker A, Kirwan CB, Miller M, Stark CE. Pattern separation in the human hippocampal CA3 and dentate gyrus. *Science*. Mar 21 2008;319(5870):1640-2. doi:10.1126/science.1152882

166. Hodgetts CJ, Voets NL, Thomas AG, Clare S, Lawrence AD, Graham KS. Ultra-High-Field fMRI Reveals a Role for the Subiculum in Scene Perceptual Discrimination. *J Neurosci*. Mar 22 2017;37(12):3150-3159. doi:10.1523/JNEUROSCI.3225-16.2017

167. Yassa MA, Mattfeld AT, Stark SM, Stark CE. Age-related memory deficits linked to circuit-specific disruptions in the hippocampus. *Proc Natl Acad Sci U S A*. May 24 2011;108(21):8873-8. doi:10.1073/pnas.1101567108